Introduction

In dryland ecosystems the biological activity and productivity are mainly constrained by water availability. Usually defined as areas where mean annual precipitation is 35% lower than mean annual potential evapotranspiration (i.e., PP/ETP <0.65) (Spinoni et al. 2015), they represent more than 40% of land surface and support around 35% of human population (Prăvălie 2016), being crucial for global sustainability achievement. By occupying the main part of Africa, Australia, Southwest of Asia, and West of America (Figure 1), drylands encompass a wide range of climatic zones including hyper-arid (PP<100 mm/year, PP/ETP < 0.05), arid (PP=100-250 mm/year, PP/ETP = 0.05-0.2), semiarid (PP=250-600 mm/year, PP/ETP < 0.2-0.5) and dry subhumid (PP= 600-1200 mm/year, PP/ETP = 0.5-0.65), regions (Spinoni et al. 2015). Overall, these regions are characterized by low mean annual precipitation which normally occur in casual and unpredictable events with large variability among years (Noy-Meir, 1973; Maestre et al., 2021). The high evaporative demand and the unpredictable water pulses modulate ecosystem structure and processes through soil moisture availability (Loik et al. 2004; Zhang et al. 2021), with strong influence on biogeochemical cycles (Ahlström et al. 2015; Osborne et al. 2022).

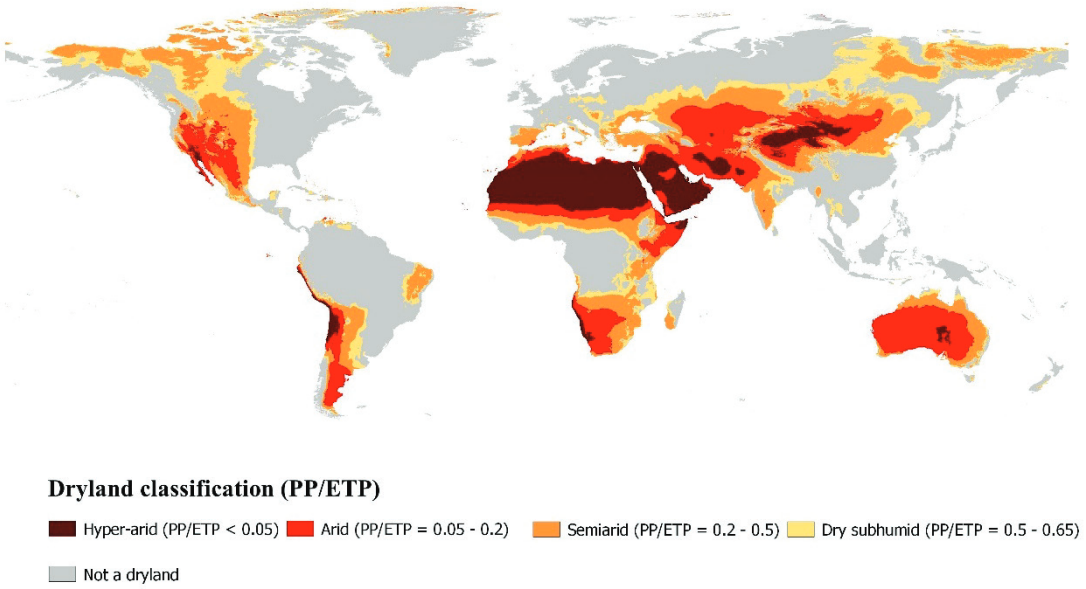

Figure 1. Dryland classification and its distribution according to FAO and Global Aridity Index database from Trabucco et al. (2018).

Several regional and global studies described a negative effect of aridification in dryland's vegetation and soils (Berdugo et al., 2020), which can be exacerbated by human activities (Li et al., 2023; Maestre et al., 2023). Despite research of the effects of global change on dryland ecosystems are increasing, there are some scientific controversies of how climatic change will affect drylands extension in the future. On the one hand it is expected that anticipated shifts on precipitation regime together with increasing air temperature will intensify climatic aridity (i.e., the difference between PP and ETP) and therefore it will promote an expansion of drylands about ~10% - ~20% of their current extent by the end of the century (Huang et al. 2016, 2017; Koutroulis 2019; Yao et al. 2020). On the other hand, CO_2 fertilization is forecasted to increase water use efficiency of vegetation (Lian et al. 2021), which will modify the atmospheric evaporative demand. In addition, reductions on soil moisture will limit evapotranspiration and water recycling for precipitation but they may enhance atmospheric moisture convergence which in the end reduces water scarcity (Zhou et al. 2021). As result, drylands might expand in some regions while they might reduce its extension in other regions (Berg and McColl 2021). This controversy emphasizes the importance of ecohydrological processes in drylands by conditioning land-atmosphere feedback and their potential relevance in a global climate change context.

Ecohydrological features and functioning of dryland ecosystems

The chronic water shortage that experience dryland ecosystems disables to sustain a continuous cover of vascular plants, affecting also soil resources and nutrient stocks (Plaza et al. 2018). Moreover, in response to the harsh environmental conditions characterizing these regions, plant species often exhibit a wide variety of phenological, morphological and physiological adaptations to cope water scarcity (Soliveres et al. 2014; Nunes et al. 2017). This results in a pool of species with a great heterogeneity in the size, shape and economic traits of the leaves and stems to reduce absorbed solar radiation and heating, and to avoid transpiration. Others have developed water and nutrient storage tissues to resist drought. There are also abundant annual forbs presenting fast biological cycles that allow them to complete their life cycle during the short periods of water availability (Klimešová et al. 2023). Perennial species of trees and shrubs presenting deep-root system to obtain soil moisture from deeper layers and minimize competition with other species are also common in drylands (Peguero-Pina et al. 2020). This broad

variety of adaptations and life forms also promote the apparition of biological relationships among species such as resources facilitation and competition that transform drylands into highly diverse and complex ecosystems (Maestre et al., 2016). For example, the above mentioned deep-rooted plants usually improve soil moisture content under their canopy by pumping up water and nutrients that can be used for other surrounding species (Sardans and Peñuelas 2014; Torres-García et al. 2022).

Reduced vegetation coverage with perennial vegetation frequently forming isolated patches interspersed with bare soil is another pervasive feature of drylands worldwide (Rietkerk et al. 2004). Vegetated patches frequently occupy most favourable positions within the landscape whereas open areas among vegetation are usually covered by physical soil crusts, stones, or low requirements organisms such us biological soil crusts (complex poikilohydric communities that live in a close relation with soil particles of the topsoil and are mainly composed by mosses, lichens, cyanobacteria, microalgae and bacteria) (Weber et al. 2016; Rodríguez-Caballero et al. 2018). As it is expected, soils in open areas are usually shallow, and show lower infiltration capacities as result of soil sealing and physical crusting processes, or the effect of disturbances such as grazing that induce soil compaction (Ravi et al. 2010; Allington and Valone 2014), or the low organic matter inputs that hinder soil development (Osborne et al. 2022). In contrast, soil under vegetated patches is usually thicker with a more developed structure promoted by the higher inputs of organic matter from plants (Ridolfi et al. 2008; Tölgyesi et al. 2020) and it presents better hydraulic properties. The magnitude of all these effects varies according to plant biomass. Moreover, the accumulation of nutrients and water in vegetated patches together with the reduction of the soil evaporation rates resulting from the higher retention capacity of these soils, and the shadow generated by the plant canopy, enhances the biological activity underplant canopy compared with surrounding open areas (D'Odorico et al. 2007; Maurice et al. 2023) and modulate biogeochemical cycles (Osborne et al. 2022). As a consequence, vegetated patches act as fertility islands in which resources cumulated (Ridolfi et al. 2008).

Different biotic and abiotic mechanism are involved in the formation of fertility island including both, biotic processes that promote resource accumulation underneath vegetation (e.g., plant biomass, roots activity, more abundant and diverse microbial communities, etc) and abiotic processes including dust trampling, rainfall interception

and steam flow, and runoff water redistribution processes (Eldidge et al., 2020). The last one is triggered by the contrasting differences on soil hydrological properties between vegetated patches and open areas (Mayor et al., 2008; Pueyo et al., 2013), and consists on the superficial redistribution of the runoff and the related nutrients generated in open areas to vegetated patches (Puigdefábregas et al. 1999; Puigdefábregas 2005; Okin et al. 2015) (Figure 2). Runoff water redistribution process promotes the creation of a complex ecohydrological source-sink system that increases water and nutrients supply for the maintenance of the biotic activity within the vegetated patch. Thus, it favours plant growth and reinforces the creation and maintenance of fertility islands (Maestre et al. 2016; Wu et al. 2023). Therefore, ecosystem functionality and dynamics are deeply related to vegetated patches and their interplay with runoff redistribution.

Figure 2. Runoff redistribution process driven by the differences in soil properties between vegetated and surrounding open areas. Open areas have shallow soil with low infiltration rates and are very efficient in runoff generation. Runoff water is infiltrated in the adjacent vegetated patches where soil structure is more developed, and infiltration is favoured. This additional supply of water and nutrients constitute a source of resources for the biotic activity of vegetation and related organisms (e.g., fauna, microfauna, soil microbes, etc) with implications on the ecosystem functioning.

Patchiness strategy in response to water scarcity

Dryland's vegetation patchiness, defined as vegetation patches size, frequency, shape and spatial distribution within the landscape, is rarely random but exhibit different configurations in which resources availability for plants are optimized to minimize environmental stress (Rietkerk et al. 2004; Berghuis et al. 2020). This self-organization process obeys the Turing instability concept (Turing 1990), in which a uniform system develops a spatial pattern based on the balance between two opposite processes that push the system: one promoting the change of the system (activation) while the other one

counterbalance this change (inhibition). An easy way to understand the Turing instability concept is to imagine a chemical reaction in which the product of the reaction acts also as inhibitor of the reaction. The final concentrations of both chemical compounds in the space (reactive and product) will depend on the balance between the speed generation the product (activation) and the speed of the product stopping the reaction (inhibition) (Rietkerk et al. 2021). Thus, in a system with no resource limitations for biological activity (i.e., without an inhibitor process) vegetation forms a uniform cover as there are no growth restrictions. As environmental stresses or "inhibition" increase (e.g., aridity, grazing, fire events, etc) and resources become more restrictive, vegetation adjusts its cover, biomass and spatial pattern according to the balance between environmental pressures and processes of resource redistribution that promoted resources accumulation on vegetated patches (e.g. runoff water redistribution; Siero, 2020).

According to the dominant operating drivers, vegetation spatial patterns have been usually classified into periodic or regular patterns (i.e., patterns that follow a determine longwave or space among plants) and irregular patterns (i.e., patterns whose do not follow a longwave) (Maestre et al. 2016). Periodic patterns are caused mainly by biotics interactions such as competition among plants for the limited water resource. Some examples include gaps of bare soil surrounded by dense vegetated patches (e.g., fairy circles on Namibia), intricate labyrinths, as well as striped or spotted patterns where vegetation is scarce and surrounded by expansive open spaces (Deblauwe et al. 2008) (Figure 3). On the other hand, irregular patterns are usually caused by abiotic drivers limiting plant growth such us topography or soil depth, and are characterized by varying patches sizes (Maestre et al. 2016). Real drylands landscapes, however, generally represent intermediate cases where the spatial pattern is the result of the interplay of abiotic constrains imposed by landscape heterogeneity (i.e., topography or soil depth), biotic interactions among plants species for resources (i.e., short-range facilitation and long-range competitive interactions for water and nutrients) and by the resulting source-sink relationships between open and vegetated areas (Sheffer et al. 2013) (Figure 3).

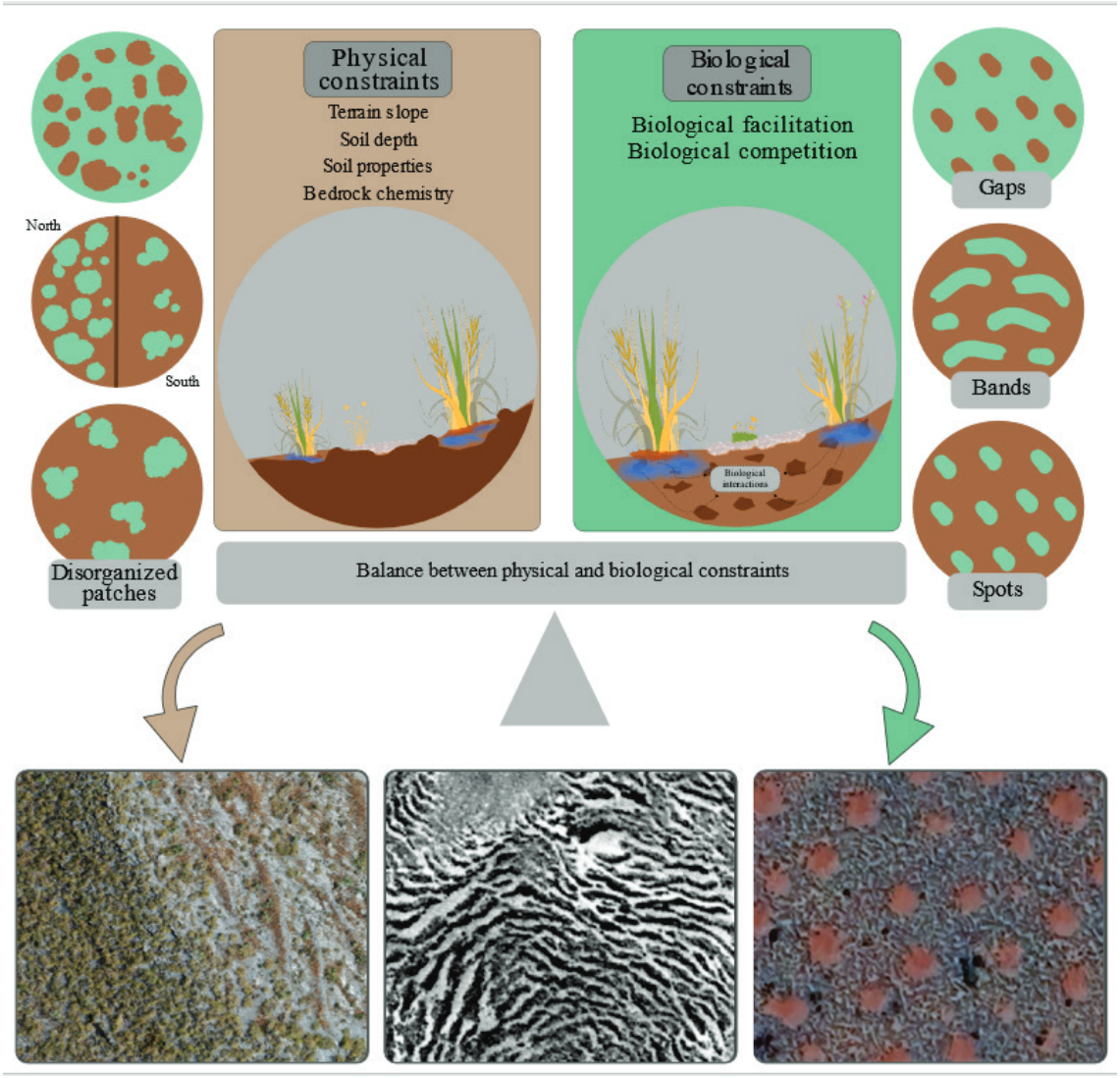

Figure 3. Balance between physical and biological factors controlling vegetation spatial pattern in drylands by conditioning water availability or plant growth. Irregular or disorganized patches usually appear when physical constrains modulate water availability while periodic patterns such as gaps, bands or spots are usually governed by biological interactions.

Indicators of the ecohydrological functioning of drylands

There exists a close link between spatial organization, environmental conditions and ecosystem functioning in drylands (Meron 2018). This, together with the high amount of freely and available remote sensing images have led to using changes vegetation spatial pattern as early warning signals for monitoring shifts in drylands functioning (Kéfi et al. 2007, 2014; Meloni et al. 2017; Génin et al. 2018). This approach is based on the concept of ecosystem stability that assumes that different biotic and abiotic relationships, modulating plant growth, promote the creation of a stable state for a given context of

environmental conditions. An increase in the environmental stress may induce changes in the different processes underlying the spatial organization of vegetation triggering the evolution of the system to a different state (Hu et al. 2022). In this context, ecosystems with regular spatial pattern clearly reflect changes on environmental pressures. They show a well-documented succession from uniform fully cover to gaps, labyrinths or stripes patches (depending on the slope of the terrain) and finally after the persistence of isolated spots of vegetation, vegetation patches completely disappear (Deblauwe et al. 2011; Meron 2018; Ghandhi et al. 2019). For ecosystems with irregular spatial patterns, the patch size distribution (number and size of plant patches) is often used as early warning signal of shifts in ecosystem structure and functioning. Under low-stress conditions, there are a wide variety of patch sizes, including large size vegetated patches, and the frequency of patch size distribution typically follows a power-law curve (Kéfi et al. 2014; Génin et al. 2018). As stress increases, larger patches tend to disappear, and the shape of the patch size distribution varies from a power law to a truncated-power law or an exponential function. This information can be also combined with additional generic indicators describing vegetated patches distribution such as their variance, skewness and near-neighbour correlation, as these indicators have been also reported to change before critical transitions between alternative stable states (Hu et al. 2022).

In addition to the analysis of the patch size structure, ecologists and hydrologists have developed different indices and metrics to incorporate ecohydrological relationships between the spatial pattern of vegetation and runoff water redistribution processes for assessing drylands functioning (e.g., Debra P.C. Peters et al., 2007; Saco et al., 2020). These include indices that aimed at evaluating the capacity of an ecosystem to connect the resources generated in the open spaces, and indices to quantify the capacity of the vegetation structure to retain this extra runoff water and related nutrients in the surrounding fertility islands (Berghuis et al. 2020). Both types of indicators, and other based on the same concept, have been applied on a wide range of drylands and conditions worldwide to effectively assess the effect of hydrological connectivity on ecosystem functioning (Moreno-De Las Heras et al. 2012; Lázaro et al. 2015; Saco et al. 2020; Calvo-Cases et al. 2021; Crompton et al. 2023). For example, Ludwig et al., 2007 proposed the landscape leakiness index (LI) which determines the potential leakiness of water and soil sediments in a landscape based on satellite images and digital elevation models (DEMs). In a nutshell, LI uses the DEM to identify flow direction and considers

vegetated patches as obstacles for runoff and estimates the potential retention of runoff and sediments within the system (ecological approach) by comparing its leaks with the maximum and minimum potential leakiness (that is with fully vegetated and without vegetation) under same topographical conditions. Other example of an ecohydrological index, with the other approach, defined in drylands, is the Flowlength (FL) proposed by Mayor et al. (2008). It also uses a DEM to derive the flow direction and vegetation maps for characterizing source-sink dynamic functioning by assuming that vegetated patches are sinks for the runoff and sediments are yielded by bare areas (sources). But, in contrast to the LI, which estimates landscape or ecosystem capacity to retain resources, FL reflects the connectivity of open spaces by determining the length of the runoff generated in each pixel, being a good indicator for runoff generation and sediment losses at different scales (hydrological approach), rather than an index of the increased resources on vegetation patches.

Although hydrological connectivity and ecosystem leakiness are related with topography and the spatial distribution of vegetated patches, they represent different process (i.e. the potential magnitude of runoff water transport within the system VS the potential capacity of the system to retain water and related resources), and should be considered together as the analysis of one of them is only partial with no information about the other one. However, they have mostly been used as separate indicators for the quantification of the hydrological connectivity between source areas within the landscape and the resource retention capacity of vegetation patches. Therefore, additional effort is needed to develop new metrics able to link processes (connectivity and retention) which condition the allocation of resources within the landscape, the magnitude of water redistribution processes and the resource retention by vegetation patches. This is key to understand the relevance of water redistribution processes for drylands functioning and to incorporate these processes in the assessment of drylands health.

The biomass of the vegetated patches has a relevant effect on the resource storage and soil properties of the fertility islands and in turn in the sink power of these patches. Thus, the monitoring is a key issue to properly characterize runoff redistribution processes in drylands. In addition, the current high availability of free remote sensing images constitutes an interesting opportunity for easily monitoring vegetation state and biomass in drylands. However, the high spatial heterogeneity characterizing dryland´s structure,

in which vegetation patches usually do not overcome pixel size joins the fact that vegetated patches are usually composed by a dynamic mixture of dry and green vegetation transforming the monitoring of biomass in dryland into a challenge (Smith et al. 2019). To overcome it, several approaches combining spectral information of vegetation with structural information from satellites have been developed at different spatial scales (Andela et al. 2013; Galidaki et al. 2017; Forkuor et al. 2020), and usually combined with field information to increase the accuracy of biomass monitoring. These approaches generally offer good results for woody vegetation such as trees (Estornell et al. 2011) or scrubs (Estornell et al. 2012; Li et al. 2015) but they frequently fail on the characterization of grasses or plants clumps (Muumbe et al. 2021) due to their complex morphology and reduced size. As consequence, the correct characterization of plant biomass in patchy grassland ecosystems is currently one of the main challenges for drylands monitoring and modelling. Thus, developing accurate methodologies able to detect variations in the photosynthetically active biomass in response to variable environmental conditions, it is of great value for monitoring the ecohydrological functioning of drylands, especially if they are easily combined with indices of spatial structure and connectivity of the landscape.

Drylands and climate change

Water limited ecosystems are one of the most threatened biomes by ongoing global change. Currently, several negative effects have been reported for drylands worldwide when aridity increases, increasing their vulnerability to desertification (Wang et al. 2022; Sun et al. 2023). According to Berdugo et al., 2022, increases in aridity promote a vegetation decline in which vegetated patches tend to expand the distance among them. An additional outcome of aridification is the decrease in the primary productivity, the photosynthetic rate of vegetation and the NDVI (Normalized Difference Vegetation Index). The reduction of plant coverage and the replacement of species for those more adapted to water scarcity (usually low size plants) diminish litter inputs into the soil exacerbating the loss of nutrients from soil by erosion (D'Odorico and Bhattachan 2012). Thus, aridification also has a negative effect on soil physicochemical properties and on biogeochemical cycles, reducing nutrient pools in the soil such as the amount of organic carbon, nitrogen, or their enzymatic activities (Delgado-Baquerizo et al. 2013; Plaza et al. 2018; Moreno-Jiménez et al. 2019). In addition, aridification also reduces soil

microbial diversity and its abundance, inducing shifts in microbial communities on soils (Delgado-Baquerizo et al. 2017) and ultimately allowing the development of fungal pathogens (Maestre et al. 2015), thus amplifying the stress for the remaining vegetation. All these negative effects of aridification on dryland soil and vegetation occur in a non-linear manner when an aridity threshold is reached (Berdugo et al. 2020, 2022a; Zhang et al. 2023). Moreover, human activities such as grazing interact with climatic drivers and can modify the occurrence of this threshold, inducing a faster breakdown of the system (Maestre et al. 2022; Li et al. 2023).

Reduced vegetation coverage in response to aridification will also suppose an increase in hydrological connectivity and runoff production that may provide local water gains for remaining vegetation, ameliorating environmental conditions for vegetation survival (Mayor et al. 2019). Conversely, hydrological connectivity can also imply water losses for vegetation when a dysfunctional spatial pattern for trapping runoff arises. Then, the effect of runoff water redistribution on ecosystem response to aridification will be modulated by the capacity of the system to retain extra runoff from open areas (Saco et al. 2020) which could be also influenced by external factors such soil properties or human disturbances. For example, by influencing soil properties related with water and nutrient dynamics, such as water holding capacity, hydraulic conductivity or soil chemistry (Muñoz et al. 2023), lithology may facilitate or hinder water and nutrient uptake for vegetation, conditioning its growth and therefore its relationship with runoff redistribution. On the other hand, human disturbances, like grazing, usually involve reductions on vegetation cover and alteration of its spatial distribution that promote soil erosion and its impoverishment and may also modify the effect of run off redistribution on plant performance (Maestre et al., 2016).

Understanding the net effect of water redistribution on the different ecosystems components and its interplay with other factors modifying water availability is currently a crucial gap to assess the effect of aridification on drylands (Pueyo et al. 2013; Okin et al. 2015; Saco et al. 2020). For example, to understand the response of vegetation to aridification we should consider the complex relationships between vegetation biomass, soil moisture availability and the related biogeochemical cycling through soil microbial activity in vegetated patches (Plaza et al. 2018; Osborne et al. 2022). Combining manipulative experiments with information recorded by remote sensors able to

encompass wide parts of the landscape could be useful to achieve this goal. Moreover, integrating information at different spatiotemporal scales is also a promising way to understand drylands dynamics because the different ecosystem components frequently have different sensitivity to aridity and other global change drivers (Berdugo et al. 2022b) and induce different responses that only can be interpreted and detected when the ecosystem is monitored at different scales.

Hypothesis

The role of runoff water redistribution for the maintenance and functioning of vegetation in drylands has been widely claimed but very few studies have measured its effect on vegetation productivity, biomass, cover, and the associated soil microbial activity. In addition, it has been hardly addressed across different environmental conditions simultaneously. The review of literature suggests that the effect of runoff water redistribution on ecosystem functioning is influenced by aridification (or other environmental disturbances) and may have two opposite effects. On the one hand, it may buffer water deficit for plants by supplying runoff water from the surrounding open areas. On the other hand, an appreciable rise in runoff may involve a loss of resources (water and nutrients) for plants if the vegetated patches are not able to trap it, amplifying environmental stresses for its survival. During the las decades, several factors influencing runoff water redistribution have been identified and some models have forecasted its role on ecosystem functioning. However, experimental evidence quantifying the effect of water redistribution on the response of dryland's ecosystems to aridification is scarce, and there are no studies evaluating the relevance of water redistribution processes for the different ecosystem components (i.e., vegetation and related soil microbial communities). Moreover, as far as we know, no study has considered simultaneously other abiotic factors, such as soil or terrain properties, that modulate the influence of water redistribution with increasing aridity.

The general hypothesis of this thesis is "runoff water redistribution plays a key role on dryland ecosystem functioning by supplying an extra input of water and nutrients for vegetation and underlying soils, but its effect is modulated by climatic conditions and by other biotic and abiotic factors conditioning the capacity of vegetated patches to trap runoff such as soil properties or by human disturbance". Accordingly, we hypothesize that the effect of runoff water redistribution buffering aridification will be stronger in more arid areas. However, this buffer effect may be constrained by the effects of soil disturbance on hydrology.

Physicochemical soil properties controlling water availability in soils, such as soil hydraulic conductivity, water holding capacity or soil temperature, are usually legacies of the underlying lithology. In addition, soil chemistry, through pH, electrical conductivity,

and ultimately nutrient availability, plays a key role on plant composition. Thus, different lithologies may involve contrasting soil moisture regimens and different plant communities under the same climatic conditions. As result, we hypothesized that the effect of aridification and the impact of runoff water redistribution on the ecosystem response to aridification (plants and the underlaying soil communities) will vary among lithologies driven by the contrasting hydrological behaviour legacy. More precisely, we expect alterations in the spatial pattern of vegetated patches in response to increased aridity that differ between contrasting lithologies. Lithology legacies also may involve different shifts on plant composition and soil microbial response with aridification as outcome of the interplay of different water availability regimes and vegetation turnover on soil carbon pools. For example, lithologies that foster the development of soils characterized by low infiltration or water retention capacity are expected to experience more pronounced impacts of increased aridity. This includes significant changes in the spatial pattern of vegetated patches with smaller and isolated vegetated patches becoming more abundant to ensure efficient water redistribution. Furthermore, higher reductions on photosynthetic biomass, photosynthetic rates and shifts on plant species composition by promoting low size species and lower microbial activity in their underlying soils are expected.

In addition, human disturbances such as grazing, or land abandonment have been reported as factors influencing the spatial arrangement of drylands because their impacts on vegetation and soils. Thus, we hypothesized that, by affecting the capacity of the ecosystem to trap and retain runoff water and related nutrients, human disturbance may play a key role determining the direction and magnitude of the effect of increased runoff generation on the survival and growth of vegetation.

Aims

The overall purpose of this thesis is to understand the effect of runoff water redistribution on the response of vegetation and underlaying soil in dryland ecosystems to aridification to elucidate if this supply of resources can buffer the expected negative effects of climate change in drylands.

For achieve that we proposed the following specifics aims:

1. To explore the potential role of the legacy of lithology on soil properties in the response of drylands to aridification by evaluating its effect in controlling the response of vegetation (cover, spatial structure, and composition) and soil microbial biomass to aridification (**Chapter I**).
2. To develop a new easily applicable measurement of the ecohydrological functionality of drylands hillslopes based on the Balance between runoff water Connectivity and potential Water Retention Capacity (BalanCR) (**Chapter II**).
3. To evaluate the relevance of runoff water redistribution and associated mechanisms as driver of drylands functioning and vulnerability to aridification induced by climate change under different disturbance conditions (**Chapter III**).
4. To develop a new non-destructive methodology for monitoring spatiotemporal dynamics of above ground (i.e., total) and green biomass of *M. tenacissima* L. plants (**Chapter IV**).
5. To experimentally explore the effect of runoff water redistribution on plants and soil functioning when aridity increases and how lithology may modulate it (**Chapter V**).

General Methodology

This PhD thesis has been developed along three different aridity gradients covered by *Macrochloa tenacissima* steppes in the Southeast of Spain, which is one of the dominant ecosystems of the Mediterranean drylands. Warming rates induced by the ongoing climate change are higher on the Mediterranean region than the global average (Lionello et al. 2014; Urdiales-Flores et al. 2023), making mediterranean dryland's excellent candidates to understand the effect of aridification on drylands.

Since each chapter has its own methodology, the purpose of the following sections is to introduce an overview about the different methods applied during this thesis, avoiding excessive details and technical terminology.

Study object: *Macrochloa tenacissima* steppes

Macrochloa tenacissima (L.) Kunth (= *Stipa tenacissima* L.), or Alpha grass steppes cover more than 32.000km^2 between the North of Africa and the South of Europe (Cortina et al. 2006; Maestre Gil et al. 2007). They span in semiarid and arid areas with high insolation rates that are associated to elevated atmospheric evaporative demand values and, in which, mean annual precipitation usually ranges between 200-400 mm, occurring mainly in autumn and spring (Aidoud 2006; Ramírez et al. 2007). These ecosystems have been traditionally strongly related with human activities as have been usually used as grazing areas and to obtain natural fibbers (Belkhir et al. 2012). Therefore, its capacity to provide ecosystem services directly affects the welfare of rural societies, especially those located in North Africa (Cortina et al. 2006). *M. tenacissima* is the predominant plant species in these steppes thanks to its wide range of adaptations to cope with water scarcity. Examples of these adaptations are the capacity of leaves to bend on themselves during dry periods to reduce stomata water losses, the lateral spread and shallow root system adapted to ensure water access, or the high proportion of necromass (i.e., dead leaves and inflorescences) composing the tussock that reduces water losses by evaporation and induces water infiltration by slowing down incoming runoff (Pugnaire et al. 1996; Maestre Gil et al. 2007; Belkhir et al. 2012; El-Abbassi et al. 2020). Together with these morphological and physiological adaptations, runoff water redistribution has been also reported as a major spatial process involved on the functioning and survival of

Macrochloa tenacissima steppes (Sanchez and Puigdefábregas 1994; Puigdefábregas et al. 1999; Puigdefábregas 2005). All these factors also allow *M. tenacissima* plants to facilitate the establishment of other plant species, contributing to the high biodiversity of these steppes (Maestre et al. 2001).

During the last decades the extension of *M. tenacissima* steppes has decreased around 63%, from the historical ~ 86.000 km^2 to the actual ~32.000 km^2 (Cortina et al. 2006). Cover reduction results from overgrazing and land degradation in north Africa and human disuse in Spain and other European countries. Despite the adaptation strategies of the vegetation inhabiting *M. tenacissima* steppes to cope with water stress, their extension is also forecasted to decrease even more by the end of the century as outcome of the current global change (Ben Mariem and Chaieb 2017).

Space for time substitution approach

To determine the effect of runoff water redistribution in vegetation and soil performance and therefore ecosystem functioning against increased aridity, we applied a space for time substitution approach. We selected three aridity gradients that encompass a wide range of aridity levels (from 0.17-0.27), see methods in Chapter I and Chapter III respectively for further details) within the natural distribution of *M. tenacissima* steppes in the region. Space for time substitution approach has been frequently used to investigate the effect of climatic shifts on ecological processes. Recently, it has been suggested that regional studies along climatic gradients should be combined with spatially distributed temporal series of information in a common statistical analysis to increase results reliability about ecological processes (Damgaard 2019). This is because this methodology also involves the associated spatial processes, and biotic and abiotic interactions, that usually appear when climatic conditions change in real ecosystems (Blois et al. 2013).

Attending the type of information obtained in each aridity gradient, they can be classified in two experimental aridity gradients over two contrasting lithologies (limestone and mica schist) where manipulative experiments and field measurements on plants and soils were conducted; and a remote sensing aridity gradient over limestone lithology where information was obtained from bibliographic reviews and remote sensing).

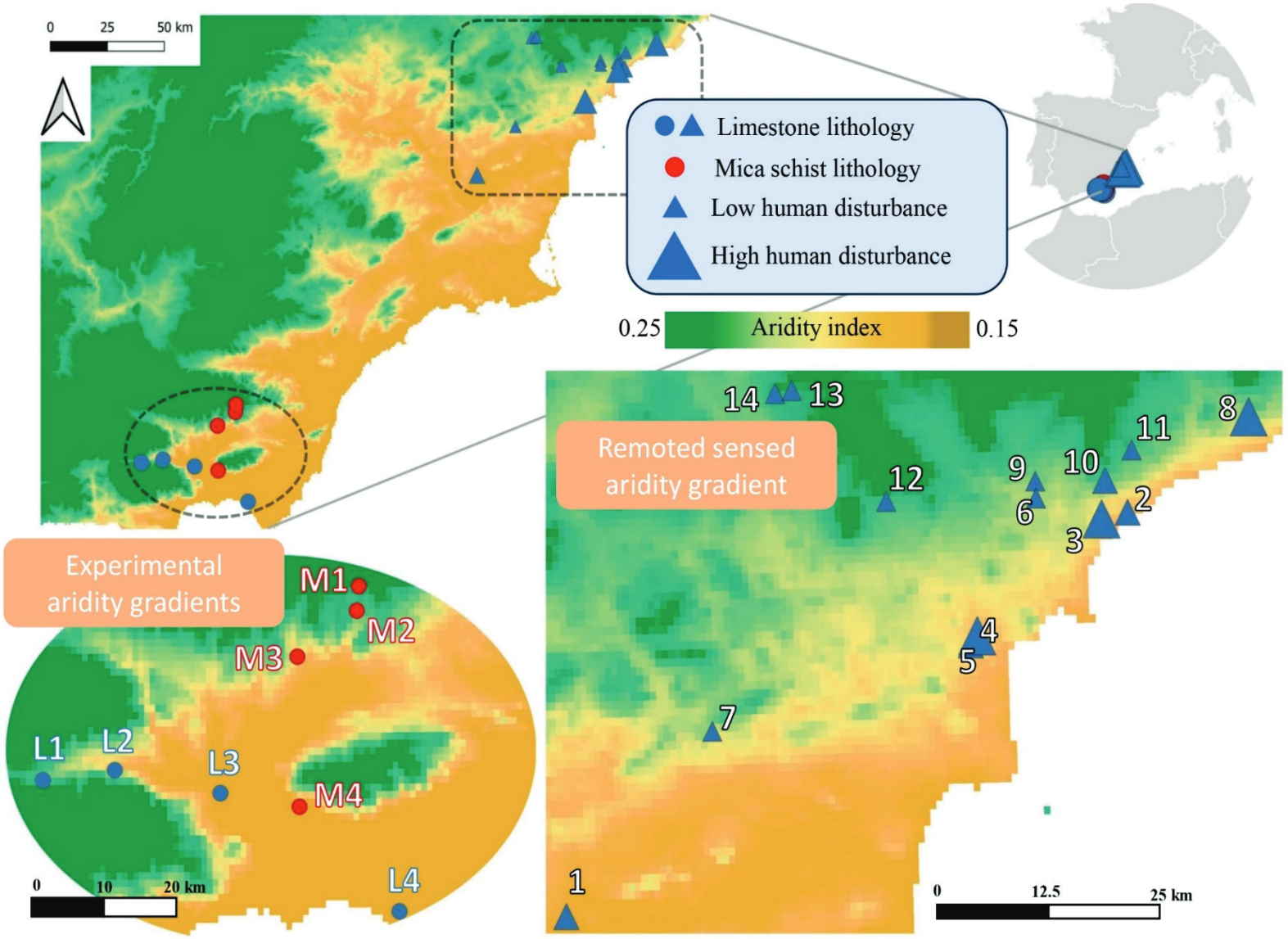

Figure 4. Experimental and remote sensing aridity gradients in the SE of Spain. Blue and red dots represent study sites composing the experimental aridity gradient on Limestone (L) and Mica schist (M) lithologies, respectively. In the remoted sensing aridity gradient, the size of the triangles indicates human disturbance obtained from Wildlife Conservation Society - WCS & CIESIN, 2005. Aridity values were obtained from Trabucco and Zomer, 2018.

Experimental aridity gradients

Two experimental altitudinal-aridity gradients, consisting in four study hillslopes each one, were settled on contrating lithologies in the province of Almería (SE Spain, Figure 4). These aridy gradients were used to conduct field measurements and manipulative experiments to assess the effect of runoff water redistribution on plant functioning and on the underliying soil response in natural *M. tenacissima* steppes in a context of aridification. The selection of two contrasted lithologies (limestone and mica schist) with contrasting hydrological properties allowed us to determine the influence of the lithology legacy modulating the runoff water redistribution effect on soil and vegetation performance under different aridity levels. The information recorded in these aridity gradients was used for the development of Chapter I, Chapter II, Chapter IV and Chapter V.

One of the experimental aridity gradient was settled on a limestone lithology (L). It spanned between 22 to 807 m.a.s.l in Sierra de Gádor, where 4 plots (hillslopes) named L4, L3, L2 and L1 (ordered from the lowest to the uppest one) were located (Figure 4). Mean annual precipitation varies between 194 mm/year (aridity index: 0.13) to 337 mm/year (aridity index: 0.22) from the lower to the upper part of the gradient. Soils in this gradient are Calcaric Regosols characterized by loam (L1) to sandy loam (L2,L3,L4) textures with moderate sand content.

The other experimental altitudinal-aridity gradient was stablished over mica schist lithology (M). Soils developed there are Eutric Regosols with sandy loam textures that are characterized by less water retention capacity than those developed on limestones lithologies. In addition, these soils on mica schist bedrock have darker colours which may induce higher soil temperatures and a faster water evaporation. Mica schist gradient spans from 298 m.a.s.l in Sierra Alhamilla (plot M4) to 1046 m.a.s.l in Sierra de los Filabres (plots M3, M2, M1) (Figure 4), with mean annual precipitation varying between 193 mm/year (aridity index= 0.17) at the lowest part to 373 mm/year at the highest upper parts (373 mm/year, aridity index= 0.27).

In both gradients, climatic conditions (i.e., mean annual temperature, mean annual precipitation and aridity index) were deeply related with altitude, with a decrease in aridity as altitude increases.

An unmanned aerial vehicle (UAV or drone) flight survey was conducted on each study plot to obtain high resolution orthoimages and Digital elevation models (DEMs) (Figure 5). These images were used to obtain high resolution vegetation maps, by supervised classification methods, to calculate vegetation patch spatial descriptors. The vegetation maps were used further in combination with the DEMs to develop a new ecohydrological indicator for potential water redistribution. Perennial plant diversity and composition were also measured in each study plot during field surveys to characterize the changes of the plant community to aridification in both gradients (see methods in Chapter I for further details).

Finally, a runoff exclusion experiment was set up in each study plot along the two experimental aridity gradients, to experimentally determine the effect of runoff water supply on the response of vegetation patches and the underlaying soil microbial activity to aridification. For that, in each plot along the gradient, 6 paired plants of *M. tenacissima* plants with a similar size were selected in different hillslope positions (upper, medium, and lower) trying to encompass a wide range of water redistribution conditions. One of the plants in the pair was settled as control while the other one was runoff excluded. Runoff exclusion was done by installing metallic sheets deeply inserted into the soil located in the upstream part of the plant acting as a shield to divert the runoff and thus prevent its infiltration in the soil under the plant (Figure 5). A total of 48 *M. tenacissima* plants and underlying soils were periodically monitored.

For plant response monitoring, a new non-destructive methodology for above ground biomass estimation based on plant volume and its spectral response was developed (see Chapter IV). Accordingly, the spectral response of vegetation under the two different treatments was also measured with a field spectroradiometer as a proxy of green biomass. Concurrently to the spectral response measurements, photosynthetic rates at leave scale were determined using a portable LICOR Li-6800 (Figure 5).

Moreover, soil organic carbon, basal respiration and substrate induced respiration, using glucose as substrate were analysed under *M. tenacissima* canopy at different time spans.

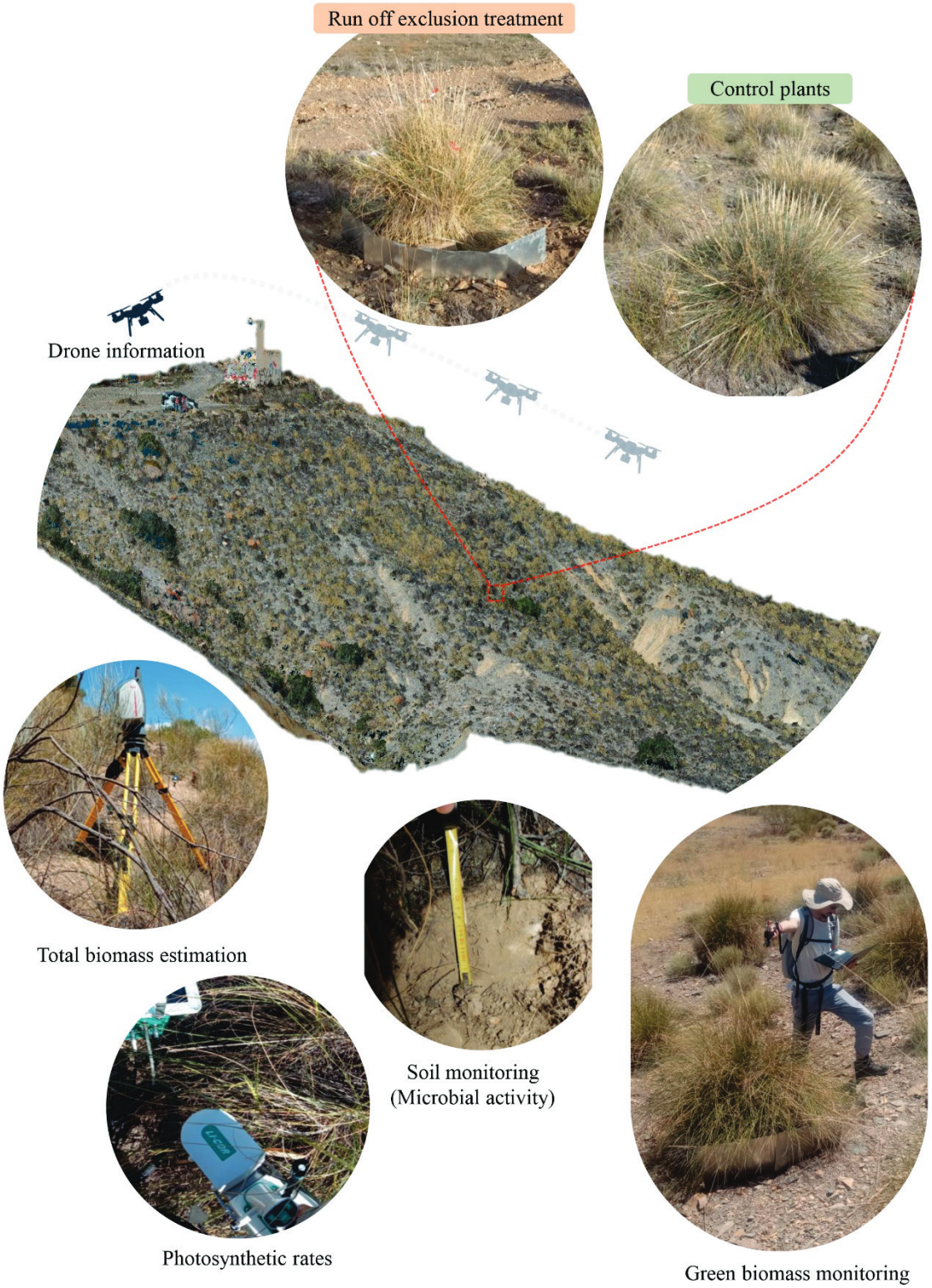

Figure 5. Schematic representation of the different information acquired in the experimental aridity gradients.

Remoted sensed aridity gradient

The remote sensed aridity gradient spanned over a ~100 km latitudinal aridity-disturbance gradient between Murcia and Alicante in the SE of Spain (Figure 4) and included 14 study hillslopes of *M. tenacissima* steppes. Aridity values ranged between 0.17-0.24 along the gradient, which correspond to 299-350 mm/year respectively. The selection of these study sites was based on the work by (Maestre and Cortina 2004) since they comprised contrasting signs of degradation, significant variations on aridity and reduced variability associated with vegetation, slope gradient and soil type. All study areas were located on limestone lithology with similar soil type (loamy-silty loam Lithic Cacіorthid).

High resolution orthoimages from the National Plan of Aerial Orthophotography of Spain (PNOA) were used to determine the study area within each study hillslope and to identify the 10 x10m SENTINEL-2 pixels corresponding to these areas. Temporal series (2016/10/01 – 2020/09/30) of the normalized difference vegetation index (NDVI) with monthly resolution were obtained for each pixel as a proxy of vegetation performance and dynamics. In these areas we also calculated the potential water redistribution, according to the new runoff water redistribution index developed in the Chapter II, and we combined it with the effect of topography on the potential incoming solar radiation, climatic information and information of Human disturbance obtained from Global Human Influence Index v2 database (Wildlife Conservation Society - WCS and CIESIN 2005) to model NDVI dinamics.

Finally, we obtained climatic predictions for the analysed aridity gradient for two contrasted Shared Socioeconomic Pathways (SSPs245 and SSPs585) and 3 climate models (GFDL-CM4, ACCESS-CM2 and IPSL-CM6A-LR) included within the 6th IPCC report (see methods in Chapter III for further details) and we applied the obtained models to predict the future response of Mediterranean *M. tenacissima* steppes.

References

Ahlström A, Raupach MR, Schurgers G, et al (2015) The dominant role of semi-arid ecosystems in the trend and variability of the land CO2 sink. Science (80-) 348:895–899. https://doi.org/10.1126/science.aaa1668

Aidoud A (2006) Les steppes arides du nord de l'Afrique. Sci Chang planétaires / Sécheresse 17(1–2):19–30

Allington GRH, Valone TJ (2014) Islands of Fertility: A Byproduct of Grazing? Ecosystems 17:127–141. https://doi.org/10.1007/s10021-013-9711-y

Andela N, Liu YY, M. Van Dijk AIJ, et al (2013) Global changes in dryland vegetation dynamics (1988-2008) assessed by satellite remote sensing: Comparing a new passive microwave vegetation density record with reflective greenness data. Biogeosciences 10:6657–6676. https://doi.org/10.5194/bg-10-6657-2013

Belkhir S, Koubaa A, Khadhri A, et al (2012) Variations in the morphological characteristics of Stipa tenacissima fiber: The case of Tunisia. Ind Crops Prod 37:200–206. https://doi.org/10.1016/j.indcrop.2011.11.021

Ben Mariem H, Chaieb M (2017) Climate change impacts on the distribution of stipa tenacissima l. Ecosystems in north african arid zone – A case study in tunisia. Appl Ecol Environ Res 15:67–82. https://doi.org/10.15666/aeer/1503_067082

Berdugo M, Delgado-Baquerizo M, Soliveres S, et al (2020) Global ecosystem thresholds driven by aridity. Science (80-) 367:787–790. https://doi.org/10.1126/science.aay5958

Berdugo M, Gaitan JJ, Delgado-Baquerizo M, et al (2022a) Prevalence and drivers of abrupt vegetation shifts in global drylands. Proc Natl Acad Sci U S A 119:1–10. https://doi.org/10.1073/pnas.2123393119

Berdugo M, Vidiella B, Solé R V., Maestre FT (2022b) Ecological mechanisms underlying aridity thresholds in global drylands. Funct Ecol 36:4–23. https://doi.org/10.1111/1365-2435.13962

Berg A, McColl KA (2021) No projected global drylands expansion under greenhouse warming. Nat Clim Chang 11:331–337. https://doi.org/10.1038/s41558-021-01007-8

Berghuis PMJ, Mayor ÁG, Rietkerk M, Baudena M (2020) More is not necessarily better: The role of cover and spatial organization of resource sinks in the restoration of patchy drylands. J Arid Environ 183:. https://doi.org/10.1016/j.jaridenv.2020.104282

Blois JL, Williams JW, Fitzpatrick MC, et al (2013) Space can substitute for time in predicting climate-change effects on biodiversity. Proc Natl Acad Sci U S A 110:9374–9379. https:/doi.org/10.1073/pnas.1220228110

Calvo-Cases A, Arnau-Rosalén E, Boix-Fayos C, et al (2021) Eco-geomorphological connectivity and coupling interactions at hillslope scale in drylands: Concepts and critical examples. J Arid Environ 186:. https://doi.org/10.1016/j.jaridenv.2020.104418

Cortina J, Maestre FT, Ramírez D (2006) Innovations in Semiarid Land Restoration. The case of Stipa tenacissima L. Steppes. In: Bautista S, Aronson J, Vallejo R V. (eds) Land restoration to combat desertification. Innovative approaches, quality control and project evaluation. Centro de Estudios Ambientales del Mediterráneo – CEAM, Paterna (Valencia) Spain, pp 121–144

Crompton O, Katul G, Lapides DA, Thompson SE (2023) Bridging structural and functional hydrological connectivity in dryland ecosystems. Catena 231:107322. https://doi.org/10.1016/j.catena.2023.107322

D'Odorico P, Bhattachan A (2012) Hydrologic variability in dryland regions: Impacts on ecosystem dynamics and food security. Philos Trans R Soc B Biol Sci 367:3145–3157. https://doi.org/10.1098/rstb.2012.0016

D'Odorico P, Caylor K, Okin GS, Scanlon TM (2007) On soil moisture-vegetation feedbacks and their possible effects on the dynamics of dryland ecosystems. J Geophys Res Biogeosciences 112:1–10. https:/doi.org/10.1029/2006JG000379

Damgaard C (2019) A Critique of the Space-for-Time Substitution Practice in Community Ecology. Trends Ecol Evol 34:416–421. https://doi.org/10.1016/j.tree.2019.01.013

Deblauwe V, Barbier N, Couteron P, et al (2008) The global biogeography of semi-arid periodic vegetation patterns. Glob Ecol Biogeogr 17:715–723. https://doi.org/10.1111/j.1466-8238.2008.00413.x

Deblauwe V, Couteron P, Lejeune O, et al (2011) Environmental modulation of self-organized periodic vegetation patterns in Sudan Published by : Wiley on behalf of Nordic Society Oikos Stable URL : https://www.jstor.org/stable/41315777 Linked references are available on JSTOR for this article : Environm. 34:990–1001

Delgado-Baquerizo M, Eldridge DJ, Ochoa V, et al (2017) Soil microbial communities drive the resistance of ecosystem multifunctionality to global change in drylands across the globe. Ecol Lett 20:1295–1305. https://doi.org/10.1111/ele.12826

Delgado-Baquerizo M, Maestre FT, Gallardo A, et al (2013) Decoupling of soil nutrient cycles as a function of aridity in global drylands. Nature 502:672–676. https://doi.org/10.1038/nature12670

El-Abbassi FE, Assarar M, Ayad R, et al (2020) A review on alfa fibre (Stipa tenacissima L.): From the plant architecture to the reinforcement of polymer composites. Compos Part A Appl Sci Manuf 128:105677. https://doi.org/10.1016/j.compositesa.2019.105677

Estornell J, Ruiz LA, Velázquez-Martí B, Fernández-Sarría A (2011) Estimation of shrub biomass by airborne LiDAR data in small forest stands. For Ecol Manage 262:1697–1703. https://doi.org/10.1016/j.foreco.2011.07.026

Estornell J, Ruiz LA, Velázquez-Martí B, Hermosilla T (2012) Estimation of biomass and volume of shrub vegetation using LiDAR and spectral data in a Mediterranean environment. Biomass and Bioenergy 46:710–721. https://doi.org/10.1016/j.biombioe.2012.06.023

Forkuor G, Benewinde Zoungrana JB, Dimobe K, et al (2020) Above-ground biomass mapping in West African dryland forest using Sentinel-1 and 2 datasets - A case study. Remote Sens Environ 236:111496. https://doi.org/10.1016/j.rse.2019.111496

Galidaki G, Zianis D, Gitas I, et al (2017) Vegetation biomass estimation with remote sensing: focus on forest and other wooded land over the Mediterranean ecosystem. Int J Remote Sens 38:1940–1966. https://doi.org/10.1080/01431161.2016.1266113

Génin A, Majumder S, Sankaran S, et al (2018) Monitoring ecosystem degradation using spatial data and the R package spatialwarnings. Methods Ecol Evol 9:2067–2075. https://doi.org/10.1111/2041-210X.13058

Ghandhi P, Iams S, Bonetti S, Silber M (2019) Vegetation pattern formation in drylands. Dryl Ecohydrol 469–509. https://doi.org/10.1007/978-3-030-23269-6_18

Hu Z, Dakos V, Rietkerk M (2022) Using functional indicators to detect state changes in terrestrial ecosystems. Trends Ecol Evol. https://doi.org/10.1016/j.tree.2022.07.011

Huang J, Li Y, Fu C, et al (2017) Dryland climate change: Recent progress and challenges. Rev Geophys 55:719–778. https://doi.org/10.1002/2016RG000550

Huang J, Yu H, Guan X, et al (2016) Accelerated dryland expansion under climate change. Nat Clim Chang 6:166–171. https://doi.org/10.1038/nclimate2837

Kéfi S, Guttal V, Brock WA, et al (2014) Early warning signals of ecological transitions: Methods for spatial patterns. PLoS One 9:10–13. https://doi.org/10.1371/journal.pone.0092097

Kéfi S, Rietkerk M, Alados CL, et al (2007) Spatial vegetation patterns and imminent desertification in Mediterranean arid ecosystems. Nature 449:213–217. https://doi.org/10.1038/nature06111

Klimešová J, Martínková J, Bartušková A, Ott JP (2023) Belowground plant traits and their ecosystem functions along aridity gradients in grasslands. Plant Soil 487:39–48. https://doi.org/10.1007/s11104-023-05964-1

Koutroulis AG (2019) Dryland changes under different levels of global warming. Sci Total Environ 655:482–511. https://doi.org/10.1016/j.scitotenv.2018.11.215

Lázaro R, Calvo-Cases A, Lázaro A, Molina I (2015) Effective run-off flow length over biological soil crusts on silty loam soils in drylands. Hydrol Process 29:2534–2544. https://doi.org/10.1002/hyp.10345

Li A, Glenn NF, Olsoy PJ, et al (2015) Aboveground biomass estimates of sagebrush using terrestrial and airborne LiDAR data in a dryland ecosystem. Agric For Meteorol 213:138–147. https://doi.org/10.1016/j.agrformet.2015.06.005

Li C, Fu B, Wang S, et al (2023) Climate-driven ecological thresholds in China's drylands modulated by grazing. Nat Sustain. https://doi.org/10.1038/s41893-023-01187-5

Lian X, Piao S, Chen A, et al (2021) Multifaceted characteristics of dryland aridity changes in a warming world. Nat Rev Earth Environ 2:232–250. https://doi.org/10.1038/s43017-021-00144-0

Lionello P, Abrantes F, Gacic M, et al (2014) The climate of the Mediterranean region: research progress and climate change impacts. Reg Environ Chang 14:1679–1684. https://doi.org/10.1007/s10113-014-0666-0

Loik ME, Breshears DD, Lauenroth WK, Belnap J (2004) A multi-scale perspective of water pulses in dryland ecosystems: Climatology and ecohydrology of the western USA. Oecologia 141:269–281. https://doi.org/10.1007/s00442-004-1570-y

Maestre F, Benito BM, Berdugo M, et al (2021) Biogeography of global drylands. New Phytol 231:540–558. https://doi.org/10.1111/nph.17395

Maestre FT, Bagousse-pinguet Y Le, Delgado-baquerizo M, et al (2022) Grazing and ecosystem service delivery in global drylands. 1–7

Maestre FT, Bautista S, Cortina J, Bellot J (2001) Potential for using facilitation by grasses to establish shrubs on a semiarid degraded steppe. Ecol Appl 11:1641–1655. https://doi.org/10.1890/1051-0761(2001)011[1641:PFUFBG]2.0.CO;2

Maestre FT, Cortina J (2004) Insights into ecosystem composition and function in a sequence of degraded semiarid steppes. Restor Ecol 12:494–502. https://doi.org/10.1111/j.1061-2971.2004.03106.x

Maestre FT, Delgado-Baquerizo M, Jeffries TC, et al (2015) Increasing aridity reduces soil microbial diversity and abundance in global drylands. Proc Natl Acad Sci U S A 112:15684–15689. https://doi.org/10.1073/pnas.1516684112

Maestre FT, Eldridge DJ, Soliveres S, et al (2016) Structure and Functioning of Dryland Ecosystems in a Changing World. Annu Rev Ecol Evol Syst 47:215–237. https://doi.org/10.1146/annurev-ecolsys-121415-032311

Maestre Gil FT, Ramírez Collantes DA, Cortina i Segarra J (2007) Ecología del esparto (Stipa tenacissima L.) y los espartales de la Península Ibérica. Ecosistemas 16:111–130

Maurice K, Laurent-Webb L, Dehail A, et al (2023) Fertility islands, keys to the establishment of plant and microbial diversity in a highly alkaline hot desert. J Arid Environ 219:. https://doi.org/10.1016/j.jaridenv.2023.105074

Mayor AG, Bautista S, Rodriguez F, Kéfi S (2019) Connectivity-Mediated Ecohydrological Feedbacks and Regime Shifts in Drylands. Ecosystems 22:1497–1511. https://doi.org/10.1007/s10021-019-00366-w

Mayor ÁG, Bautista S, Small EE, et al (2008) Measurement of the connectivity of runoff source areas as determined by vegetation pattern and topography: A tool for assessing potential water and soil losses in drylands. Water Resour Res 44:. https://doi.org/10.1029/2007WR006367

Meloni F, Granzotti CRF, Bautista S, Martinez AS (2017) Scale dependence and patch size distribution: Clarifying patch patterns in Mediterranean drylands. Ecosphere 8:. https://doi.org/10.1002/ecs2.1690

Meron E (2018) From Patterns to Function in Living Systems: Dryland Ecosystems as a Case Study. Annu Rev Condens Matter Phys 9:79–103. https://doi.org/10.1146/annurev-conmatphys-033117-053959

Moreno-De Las Heras M, Saco PM, Willgoose GR, Tongway DJ (2012) Variations in hydrological connectivity of Australian semiarid landscapes indicate abrupt changes in rainfall-use efficiency of vegetation. J Geophys Res Biogeosciences 117:1–15. https://doi.org/10.1029/2011JG001839

Moreno-Jiménez E, Plaza C, Saiz H, et al (2019) Aridity and reduced soil micronutrient availability in global drylands. Nat Sustain 2:371–377. https://doi.org/10.1038/s41893-019-0262-x

Muñoz R, Enríquez M, Bongers F, et al (2023) Lithological substrates influence tropical dry forest structure, diversity, and composition, but not its dynamics. Front For Glob Chang 6:1–11. https://doi.org/10.3389/ffgc.2023.1082207

Muumbe TP, Baade J, Singh J, et al (2021) Terrestrial laser scanning for vegetation analyses with a special focus on savannas. Remote Sens 13:1–31. https://doi.org/10.3390/rs13030507

Noy-Meir (1973) Desert Ecosystems:Environment and producers. Annu Rev Ecol Evol Syst 25–51

Nunes A, Köbel M, Pinho P, et al (2017) Which plant traits respond to aridity? A critical step to assess functional diversity in Mediterranean drylands. Agric For Meteorol 239:176–184. https://doi.org/10.1016/j.agrformet.2017.03.007

Okin GS, De Las Heras MM, Saco PM, et al (2015) Connectivity in dryland landscapes: Shifting concepts of spatial interactions. Front Ecol Environ 13:20–27. https://doi.org/10.1890/140163

Osborne BB, Bestelmeyer BT, Currier CM, et al (2022) The consequences of climate change for dryland biogeochemistry. New Phytol 236:15–20. https://doi.org/10.1111/nph.18312

Peguero-Pina JJ, Vilagrosa A, Alonso-Forn D, et al (2020) Living in drylands: Functional adaptations of trees and shrubs to cope with high temperatures and water scarcity. Forests 11:1–23. https://doi.org/10.3390/F11101028

Peters DPC, Bestelmeyer BT, Turner MG (2007) Cross-scale interactions and changing pattern-process relationships: Consequences for system dynamics. Ecosystems 10:790–796. https://doi.org/10.1007/s10021-007-9055-6

Plaza C, Zaccone C, Sawicka K, et al (2018) Soil resources and element stocks in drylands to face global issues. Sci Rep 8:1–8. https://doi.org/10.1038/s41598-018-32229-0

Prăvălie R (2016) Drylands extent and environmental issues. A global approach. Earth-Science Rev 161:259–278. https://doi.org/10.1016/j.earscirev.2016.08.003

Pueyo Y, Moret-Fernández D, Saiz H, et al (2013) Relationships Between Plant Spatial Patterns, Water Infiltration Capacity, and Plant Community Composition in Semi-arid Mediterranean Ecosystems Along Stress Gradients. Ecosystems 16:452–466. https://doi.org/10.1007/s10021-012-9620-5

Pugnaire FI, Haase P, Incoll LD, Clark SC (1996) Response of the Tussock Grass Stipa tenacissima to Watering in a Semi-Arid Environment. Funct Ecol 10:265. https://doi.org/10.2307/2389852

Puigdefábregas J (2005) The role of vegetation patterns in structuring runoff and sediment fluxes in drylands. Earth Surf Process Landforms 30:133–147. https://doi.org/10.1002/esp.1181

Puigdefábregas J, Sole A, Gutierrez L, et al (1999) Scales and processes of water and sediment redistribution in drylands: Results from the Rambla Honda field site in Southeast Spain. Earth Sci Rev 48:39–70. https://doi.org/10.1016/S0012-8252(99)00046-X

Ramírez DA, Bellot J, Domingo F, Blasco A (2007) Stand transpiration of Stipa tenacissima grassland by sequential scaling and multi-source evapotranspiration modelling. J Hydrol 342:124–133. https://doi.org/10.1016/j.jhydrol.2007.05.018

Ravi S, Breshears DD, Huxman TE, D'Odorico P (2010) Land degradation in drylands: Interactions among hydrologic-aeolian erosion and vegetation dynamics. Geomorphology 116:236–245. https://doi.org/10.1016/j.geomorph.2009.11.023

Ridolfi L, Laio F, D'Odorico P (2008) Fertility island formation and evolution in dryland ecosystems. Ecol Soc 13:. https://doi.org/10.5751/ES-02302-130105

Rietkerk M, Bastiaansen R, Banerjee S, et al (2021) Evasion of tipping in complex systems through spatial pattern formation. Science (80-) 374:. https://doi.org/10.1126/science.abj0359

Rietkerk M, Dekker SC, De Ruiter PC, Van De Koppel J (2004) Self-organized patchiness and catastrophic shifts in ecosystems. Science (80-) 305:1926–1929. https://doi.org/10.1126/science.1101867

Rodríguez-Caballero E, Chamizo S, Roncero-Ramos B, et al (2018) Runoff from biocrust: A vital resource for vegetation performance on Mediterranean steppes. Ecohydrology 11:1–13. https://doi.org/10.1002/eco.1977

Saco PM, Rodríguez JF, Moreno-de las Heras M, et al (2020) Using hydrological connectivity to detect transitions and degradation thresholds: Applications to dryland systems. Catena 186:104354. https://doi.org/10.1016/j.catena.2019.104354

Sanchez G, Puigdefábregas J (1994) Interactions of plant growth and sediment movement on slopes in a semi-arid environment. Geomorphology 9:243–260. https://doi.org/10.1016/0169-555X(94)90066-3

Sardans J, Peñuelas J (2014) Hydraulic redistribution by plants and nutrient stoichiometry: Shifts under global change. Ecohydrology 7:1–20. https://doi.org/10.1002/eco.1459

Sheffer E, von Hardenberg J, Yizhaq H, et al (2013) Emerged or imposed: A theory on the role of physical templates and self-organisation for vegetation patchiness. Ecol Lett 16:127–139. https://doi.org/10.1111/ele.12027

Siero E (2020) Resolving soil and surface water flux as drivers of pattern formation in Turing models of dryland vegetation: A unified approach. Phys D Nonlinear Phenom 414:132695. https://doi.org/10.1016/j.physd.2020.132695

Smith WK, Dannenberg MP, Yan D, et al (2019) Remote sensing of dryland ecosystem structure and function: Progress, challenges, and opportunities. Remote Sens Environ 233:. https://doi.org/10.1016/j.rse.2019.111401

Soliveres S, Maestre FT, Bowker MA, et al (2014) Functional traits determine plant co-occurrence more than environment or evolutionary relatedness in global drylands. Perspect Plant Ecol Evol Syst 16:164–173. https://doi.org/10.1016/j.ppees.2014.05.001

Spinoni J, Vogt J, Naumann G, et al (2015) Towards identifying areas at climatological risk of desertification using the Köppen-Geiger classification and FAO aridity index. Int J Climatol 35:2210–2222. https://doi.org/10.1002/joc.4124

Sun C, Feng X, Fu B, Ma S (2023) Desertification vulnerability under accelerated dryland expansion. L Degrad Dev 34:1991–2004. https://doi.org/10.1002/ldr.4584

Tölgyesi C, Török P, Hábenczyus AA, et al (2020) Underground deserts below fertility islands? Woody species desiccate lower soil layers in sandy drylands. Ecography (Cop) 43:848–859. https://doi.org/10.1111/ecog.04906

Torres-García MT, Oyonarte C, Cabello J, et al (2022) The potential of groundwater-dependent ecosystems to enhance soil biological activity and soil fertility in drylands. Sci Total Environ 826:. https://doi.org/10.1016/j.scitotenv.2022.154111

Trabucco A, Zomer RJ (2018) Global Aridity Index and Potential Evapo-Transpiration (ET0) Climate Database v2. CGIAR Consortium for Spatial Information (CGIAR-CSI). Publ online, available from CGIAR-CSI GeoPortal https://cgiarcsi.community

Turing AM (1990) The chemical basis of morphogenesis. Bull Math Biol 52:153–197. https://doi.org/10.2307/1292482

Urdiales-Flores D, Zittis G, Hadjinicolaou P, et al (2023) Drivers of accelerated warming in Mediterranean climate-type regions. npj Clim Atmos Sci 6:. https://doi.org/10.1038/s41612-023-00423-1

Wang L, Jiao W, MacBean N, et al (2022) Dryland productivity under a changing climate. Nat Clim Chang 12:981–994. https://doi.org/10.1038/s41558-022-01499-y

Weber B, Büdel B, Belnap J (2016) Biological soil crusts: An organizing principle in drylands. Springer

Wildlife Conservation Society - WCS, CIESIN C for IESIN- (2005) Last of the Wild Project, Version 2, 2005 (LWP-2): Global Human Influence Index (HII) Dataset (Geographic). Palisades, New York: NASA Socioeconomic Data and Applications Center (SEDAC). Columbia Univ.

Wu L, Chen H, Chen D, et al (2023) Soil biota diversity and plant diversity both contributed to ecosystem stability in grasslands. Ecol Lett 26:858–868. https://doi.org/10.1111/ele.14202

Yao J, Liu H, Huang J, et al (2020) Accelerated dryland expansion regulates future variability in dryland gross primary production. Nat Commun 11:1–10. https://doi.org/10.1038/s41467-020-15515-2

Zhang F, Biederman JA, Dannenberg MP, et al (2021) Five Decades of Observed Daily Precipitation Reveal Longer and More Variable Drought Events Across Much of the Western United States. Geophys Res Lett 48:1–11. https://doi.org/10.1029/2020GL092293

Zhang J, Feng Y, Maestre FT, et al (2023) Water availability creates global thresholds in multidimensional soil biodiversity and functions. Nat Ecol Evol 7:1002–1011. https://doi.org/10.1038/s41559-023-02071-3

Zhou S, Williams AP, Lintner BR, et al (2021) Soil moisture–atmosphere feedbacks mitigate declining water availability in drylands. Nat Clim Chang 11:38–44. https://doi.org/10.1038/s41558-020-00945-z

Chapter I:

Lithology modulates the response of water limited Mediterranean ecosystems to aridification.

Borja Rodríguez-Lozano[1,2], Emilio Rodríguez-Caballero[1,2], Juan F. Martínez-Sánchez[1,2], Esther Giménez-Luque[1,2], Yolanda Cantón[1,2]

[1] Agronomy Department, University of Almería, 04120 Almería, Spain.

[2] Research Centre for Scientific Collections from the University of Almería (CECOUAL), 04120, Almería, Spain.

Published: Landscape ecology (2023). DOI:

https://doi.org/10.1007/s10980-023-01767-y

Abstract

Context *Macrochloa tenacissima* (L.) Kunth (= *Stipa tenacissima* L.), also defined as Alpha grass steppes, form the main dryland ecosystems throughout the Mediterranean region. Recent studies suggest that ongoing climate change will lead to a sequence of changes in them, including modifications in the composition of vegetation and reduction in vegetation cover and biomass, which will diminish plant derived organic inputs into the soil. These changes are expected to affect the spatial arrangement of vegetation and the ecosystem's water-nutrient balance, as well as the microbial populations in the underlying soil. In addition, the lithological legacy affecting soil hydrological properties might modulate the effects of aridity.

Objectives With this study, we wanted to evaluate the interactive effects of the lithological legacy on soil water availability and aridification on vegetation cover, spatial structure, and composition, and on soil microbial biomass.

Methods We combined field data, including plant composition and soil physicochemical and biological properties, with unmanned aerial vehicle (UAV) images collected at eight study sites along two different altitudinal-aridity gradients with contrasting lithologies in a space-for-time substitution approach to explain the role of lithological legacies on soil properties in aridification. High-resolution UAV images were used to determine the vegetation cover and three spatial metrics related with the hydrological connectivity within the study areas. Soil microbial biomass was estimated using the substrate-induced respiration method.

Results Aridification was critical to explaining changes in vegetation coverage, diversity, richness, and spatial distribution, reducing plant cover, and promoting dominance of small round isolated vegetation patches. By modulating soil physicochemical properties, lithology interacted with aridity controlling the variations in plant composition and the changes in soil microbial biomass along the altitudinal aridity gradients. This may have also affected nutrient cycling, thus determining the response of the ecosystem to aridification.

Keywords: Unmanned aerial vehicle, Vegetation, Spatial pattern, *Stipa tenacissima*, Soil microbial biomass, Dryland, Spain

Introduction

Drylands comprising hyper-arid, arid, semiarid and dry subhumid regions cover more than 41% of the terrestrial land surface (Prăvălie 2016) and support almost 40% of the human population (Cherlet et al. 2018), who directly benefit from their ecosystem services and goods (Lu et al. 2018; Liao et al. 2020). Drylands are defined as water-limited ecosystems (Noy-Meir 1973), where the frequency, duration and intensity of rainfall govern vegetation and soil biological activity (Ackerly 2003; Weltzin et al. 2003; Zhang et al. 2016; Brandt et al. 2019; Peguero-Pina et al. 2020). The variety of dryland biomes (e.g., arid steppes, grasslands, tropical and subtropical savannas, dry forests, etc.), their complex topography (Suggitt et al. 2018), heterogenous lithology and long historic human land use (Bonkoungou 2001) have transformed them into very heterogeneous ecosystems that have become biodiversity hotspots (Maestre et al. 2021). In spite of the wide diversity of plants and high endemism rates, drylands usually have sparse vegetation cover forming patches comprised of various plant species (D'Odorico and Bhattachan 2012; Ghandhi et al. 2019). Plants are known to improve their surrounding environment, especially soil, by affecting the soil organic nutrient pool. Moreover, plant roots and stems modify soil surface properties, creating preferential flows. Along with the effect of increasing organic matter, this improves soil porosity and structure, enhancing infiltration and water storage (Pugnaire et al. 2011). Vegetation patches are therefore considered fertile islands that act as runoff sinks compared to open areas, which are frequently covered by stones or physical and biological soil crusts, all of them with lower infiltration rates than vegetated areas (Mayor et al. 2008; Cantón et al. 2011). During most rainfall events, runoff is generated in open areas and redistributed to vegetation where run-on is infiltrated, promoting vegetation survival, growth, and development (Ludwig et al. 2005; Rodríguez-Caballero et al. 2018). This greater water availability in soil under vegetation patches also favours soil microbial activity (D'Odorico et al. 2007; Kaouthar and Chaieb 2009), thus intensifying nutrient cycling from litter and other vegetation inputs. As a result, most drylands can be considered complex coupled ecohydrological systems in which the spatial distribution of vegetated and unvegetated areas modulates water and nutrient redistribution by runoff, while at the same time, water redistribution drives ecosystem functionality (Okin et al. 2015; Bautista and Mayor 2021).

Aridification in water-limited ecosystems leads to abrupt changes in multiple ecosystem attributes, including less productive vegetation, cover and biomass, and shifts in plant composition (Berdugo et al. 2020). Expected reduction in plant-derived organic soil inputs able to alter microbial activity and nutrient cycling will intensify environmental stress on vegetation. Moreover, as vegetation cover declines, small and isolated vegetated patches are also expected to become more abundant, and their spatial arrangement will be modified (Meloni et al 2019). This may have important implications for ecohydrological connectivity and ecosystem functioning (Lin et al. 2010; Génin et al. 2018), thus affecting its resilience (Mayor et al. 2013).

Several important soil properties modulating water availability are a legacy of the lithology or parent material. Thus, in addition to climatic drivers, lithology is another major environmental factor with important implications for dryland vegetation composition, structure, and functioning. For example, by affecting soil texture, porosity, or structure (Martínez-Hernández et al. 2017), lithology indirectly controls plant soil moisture availability dynamics and soil microbial activity (Regüés et al. 2017; Dacal et al. 2022), which in turn affect carbon input into the soil, microbial diversity and composition (Moyano et al. 2013; Company et al. 2022), and nutrient cycling. Thus, the lithological legacy may buffer or amplify the potential cascading effects of climate change induced by aridification in drylands. However, the effects of the interaction between these key drivers on vegetation composition, structure, functioning and soil microbial biomass in drylands have not been analysed, or considered in studies on the response of these ecosystems to climate change.

Although dryland ecosystems properties and processes (e.g., vegetation composition, cover and structure, soil microbial composition and activity, biogeochemical cycling, etc.) may respond differently to low water availability, they are closely interconnected. Thus, the effects of aridification in one of them may trigger changes in others, which hinders analysis of dryland response to climate change. On this basis, to properly evaluate the influence of lithology on dryland ecosystems' response to climate change, the most relevant ecosystem properties and processes should be quantified simultaneously under different climatic and environmental conditions. This can be done by the synergistic use of traditional field and laboratory work with novel remote sensing approaches (Rodríguez-Caballero et al. 2022; Berdugo et al. 2020). Such techniques provide high

spatial resolution information able to reflect the importance of local environmental factors without losing the valuable information contained at landscape scale. For example, while soil properties and vegetation composition can be determined in the field, remote sensing imagery can provide continuous information over larger areas of the territory, enabling proper assessment of vegetation performance, coverage, and spatial distribution (Smith et al. 2019). However, the spatial resolution of most satellite products is very often too coarse for accurate characterization of the inherent spatial heterogeneity of drylands, where vegetation patches tend to be smaller than pixel size (Dawelbait and Morari 2008; Smith et al. 2019). Unmanned Aerial Vehicle (UAV) imagery can overcome this limitation by increasing the spatial resolution from meters to centimetres, precisely characterizing the shape and size of vegetated patches (Kaneko and Nohara 2014; Al-Ali et al. 2020; Getzin et al. 2022). This is very useful in detecting changes in vegetation response to environmental drivers.

In this study, we proposed a space-for-time substitution (SFT) design along altitudinal-aridity gradients on contrasting lithologies to evaluate the hypothesis that "Lithological legacy modulates the resilience of dryland vegetation and underlying soil communities to aridification by modifying the soil environment (e.g., water availability, nutrient pools, etc.)." Our objective was therefore to explore the potential role of the legacy of lithology on soil properties in the response of drylands to climate change by evaluating its effect in controlling vegetation response properties (cover, spatial structure, and composition) and soil microbial biomass to aridification.

Methods

Spatial framework and study areas

We focused our study on semiarid steppes dominated by *Macrochloa tenacissima* (L.) Kunth (previously *Stipa tenacissima* L.) or Alpha grass steppes, hereinafter *M. tenacissima*. They are one of the most representative ecosystems in the Mediterranean basin, covering more than 32.000 km^2 between the Northwest of Africa and Spain, including a wide range of soil properties and lithologies, predominantly limestone and mica schist (Aidoud 2006; Maestre et al. 2007). *M. tenacissima* is a grass well adapted to survive under the harsh environmental conditions that characterise drylands regions such as long periods of water stress, high solar insolation and shallow soils (Ramírez et al.

2007a). The plant structure of *M. tenacissima* together with the huge number of dead leaves in the tussock, promote the interception of runoff fluxes, making the ecohydrological connectivity a key process regulating the growth and survival of *M. tenacissima* (Puigdefábregas et al. 1999; Puigdefábregas 2005; Rodríguez-Caballero et al. 2018).

Eight hillslopes along two altitudinal-aridity gradients on two different lithologies in the province of Almería (Southeast of Spain) were selected as study areas (Fig. 1). The selected hillslopes include the natural climatic range of distribution of *M. tenacissima* in the region. One of the altitude gradients was settled over limestone soils and the other one on soils developed from a mica schist bedrock, which are usually foliated rocks that promote the formation of soils with coarse fragments and lower water holding capacities than the limestone soils. Each altitudinal-aridity gradient included four study areas (Fig. 1) and all of them were characterised by low developed and shallow soils. The study areas (or plots) on the limestone gradient (L) are located between 22 m.a.s.l (Las Amoladeras, plot L4) and 807 m.a.s.l (Sierra de Gádor, plots L3, L2, L1) while plots on the mica schist gradient (M) span between 298 to 1046 m.a.s.l., from Sierra Alhamilla (plot M4) to Sierra de Filabres (plots M3, M2, M1) (Fig. 1, Table 1). Mean annual precipitation, mean annual temperature and the mean f maximum annual temperature were obtained for each study area (Table 1) using the Climatic Atlas from Agencia Estatal de Meteorología (AEMET 250 m of spatial resolution, http:// agroc limap. aemet.es), which offers interpolated data of mean temperature and mean precipitation for all Spain using records from 1971 to 2000. Aridity index (AI; ratio between mean annual precipitation and mean annual evapotranspiration, dimensionless) was obtained from Global Aridity Index Dataset (30 arc seconds of spatial resolution [~ 1 km at the equator]; Trabucco and Zomer 2018). Aridity index shows higher values in less arid areas (higher altitude) and decreases as aridity increases, ranging between 0.17–0.27 in the limestone lithology altitudinal gradient and between 0.13–0.22 in the mica schist gradient (Table 1).

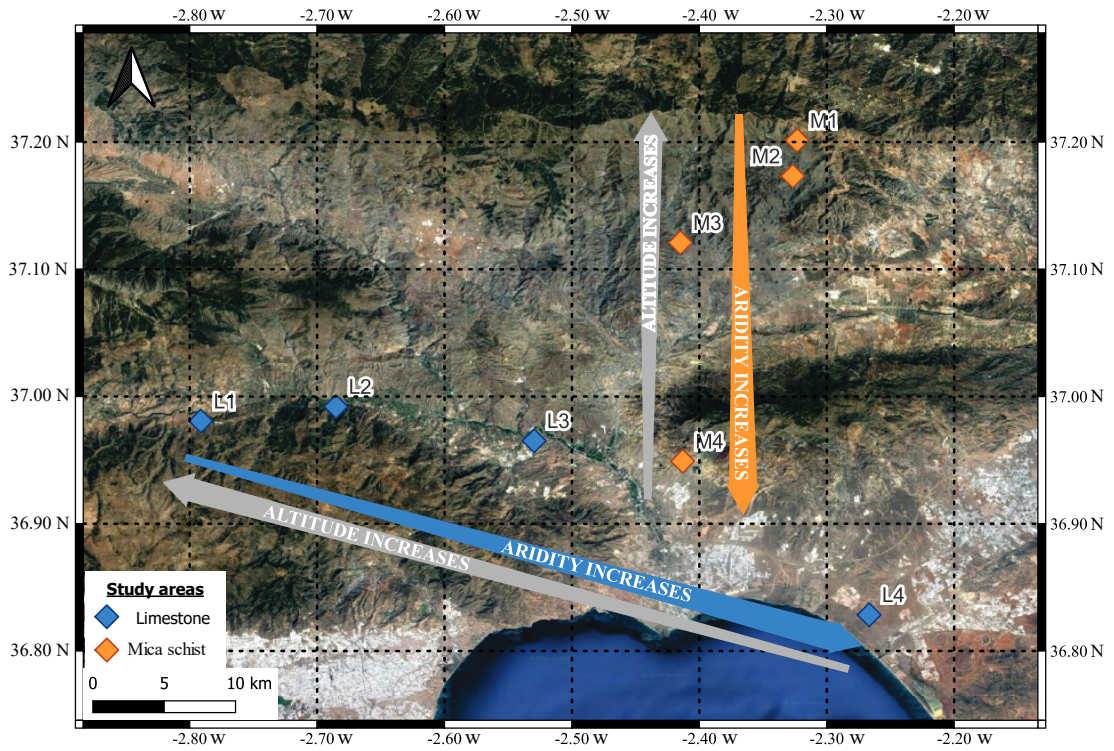

Fig. 1 Location of study areas in province of Almeria (Southeast of Spain). Dots symbolize study areas over different lithologies (orange for mica schist and blue for limestone lithology). Arrows indicate aridity and altitude gradients, being aridity index higher (less aridity and therefore more precipitation) in the areas with higher altitude. Background image of land surface was obtained from © Google Earth 2022.

Gradient	Study area	Altitude (m.a.s.l.)	Tmax (ºC)	Tmean (ºC)	PP (mm)	AI
Limestone	L1	807	19.5	14.6	337	0.22
Limestone	L2	652	21.2	16.2	269	0.19
Limestone	L3	258	23.0	17.9	215	0.17
Limestone	L4	22	23.6	19.5	194	0.13
Mica schist	M1	1046	23.5	15.4	373	0.27
Mica schist	M2	764	23.8	16.2	322	0.21
Mica schist	M3	620	23.6	16.6	243	0.18
Mica schist	M4	298	23.2	18	193	0.17

Table 1 Climatic characterization of study areas where Tmax, Tmean and PP are the annual mean of maximum temperatures (°C), the mean annual temperature (°C) and the mean annual precipitation (mm) during 1981–2010, respectively. AI is the Aridity Index (dimensionless) obtained from (Trabucco and Zomer 2018). Note that higher values of AI reflect more humid conditions and therefore less aridity. Altitude is expressed in meters above sea level (m.a.s.l.).

Vegetation cover and spatial pattern with UAV image

High resolution UAVs images were acquired for each study area using a Mavic Pro 2—DJI drone with a Hasselblad L1D-20C RGB (20 Megapixels) camera at 80 m above ground surface. The numbers of pictures necessary to characterise each plot depended on hillslope length, ranging between 146 and 450 to ensure a 90% of longitudinal overlap and 70% of lateral overlap between photographs. Individual images were merged to create a very detailed orthoimage of each plot using PIX4Dmapper software. Images were georeferenced by using the coordinates of a set of ground control points, that varied from 4 to 6 depending on the plot size and recorded using a Leyca Zeno 20 GPS with 1 cm of accuracy.

Detailed maps of vegetation and open soil were built from the RGB orthoimages at 20 cm of spatial resolution by applying the supervised classification algorithm of Maximum likelihood using ArcMap 10.5. To do this, we identified 150 training points of each of the two cover classes (vegetated patches and open soil patches) by visual interpretation of the orthoimages from each study area. Additional sets of 50 points per class (validation points) were identified at each site and later used to build the confusion matrices to calculate the kappa indices and the overall accuracy of the classifications. Classification maps with kappa index lower than 0.9 were discarded and new training points were acquired to ensure a precise mapping of both cover classes. Resulting classification maps were used to calculate the total cover of perennial vegetation and open spaces as the sum of all pixels classified as vegetation and bare soil respectively, and to calculate three spatial indices related with the level of aggregation, the size and the shape of the patches of each class: (i) the aggregation index, which is related with the adjacencies of each patch and reflects how close are the patches of the same class each other, thus representing the connectivity between them. For example, in a natural system, a high aggregation index for open spaces means that runoff sources are well connected; (ii) the mean area of all patches, which is an area and edge metric associated with the composition of the landscape reflecting the patches size. As water availability conditions become more stressful, the mean area of vegetated patches is expected to be lower as outcome of competition for runoff water between plants; and (iii) the patch circularity, which is a shape metric related with the patch's compactness, defined as the ratio between patch area and the smallest circumscribing circle of the corresponding patch. Overall, the shape of vegetated patches is more irregular when competition for resources between different

patches is lower whereas they tend to form isolated circular patches as aridity increases (Deblauwe et al. 2011), thus lower values of the circularity index are expected in wettest high-altitude areas. Spatial distribution indices at the class level (average values of vegetation and soil patches) were calculated for each site using the Landscapemetrics package in R (R version 4.0.2), see (Hesselbarth et al. 2019) for further details about indices calculation and description.

Perennial vegetation composition, richness, diversity, and evenness

Composition, richness, diversity, and evenness of the different study sites were measured during a field survey in the 8 study areas. In each study area we delimited three 5 × 5 m sampling plots on a transect along the hillslope. We identified and counted all individuals of the different perennial plant species appearing within each plot. Relative abundance of each of the perennial plant species found in each plot was calculated by using Eq. (1) before further analysis:

$$Relative\ abundance = \frac{n_i}{N_T} \quad \text{(Eq.1)}$$

where n_i is the number of individuals of each species recorded in each plot and N_T is total number of individuals recorded on the plot.

In addition, for each study area, we calculated three biodiversity indices per plot: species richness (S), Shannon–Wiener index (H′) and Pielou index (J). Species richness (S) represents the number of species detected in each plot without considering species abundances (Moore 2013). Shannon–Wiener index (H′) determine how similar are the abundances of different species in a community and was computed following Eq. (2) (Shannon 1948):

$$H' = -\sum_{i=1}^{S} p_i \ln (p_i) \quad \text{(Eq.2)}$$

where H′ is the Shannon–Wiener index, S is the number of species, p_i is the proportion of one species in the community. Pielou index (J) represents the evenness of species and was calculated following Eq. (3) (Pielou 1966):

$$J = \frac{H'}{\ln(S)} \quad \text{(Eq.3)}$$

where J is the Pielou Index, H’ is the Shannon–Wiener index and S is the number of species or richness.

Soil sampling and analysis

Soil sampling was conducted under *M. tenacissima* canopies. In each study area, six *M. tenacissima* plants were selected along the hillslope trying to encompass the plant size range in the corresponding study area (48 soil samples in total). For each plant, composed soil samples from the first 5 cm depth were taken considering both sides (left and right side) of each tussock to avoid orientation bias in soil properties. Soil samples were immediately transported in plastic bags to the laboratory at the University of Almeria, where they were air dried, sieved at 2 mm and stored at 4 °C for further analysis. Soil bulk density was also measured in the field, under 5 different plants by using standard coring technique.

In each soil sample we measured the following soil properties: soil texture using Robinson's pipette method (Gee and Or 2002), soil organic carbon content (SOC) using the Walkley–Black protocol modified by (Mingorance et al. 2007), soil water retention capacity at 0.33 atm (or field capacity, WC0.33) and 15 atm (or wilting point, WC15) suction pressures using Richard's membrane method (Klute and Klute 1986). Available water for plants (AW) in the upper 5 cm, was determined by the difference between WC0.33 and WC15. The substrate induction respiration method (SIR; Bailey et al. 2002) was also applied as a proxy of the microbiological biomass (MB) by using the Q-Box SR1LP Soil Respiration Package (https:// qubit biolo gy. com/). As MB usually presents higher spatial heterogeneity than the rest of studied soil properties, we analysed 3 replicates per soil sample. A preincubation, consisting in keeping the sample dry during 24 h at room temperature within a 100 ml laboratory sealed bottle, was performed to allow soil microbial organisms to recover their activity after cold storage. We prepared 15 g of soil per replicate and added 0.15 g of D- (+)-glucose dissolved in 1.12 ml of distilled water as substrate (dissolution of 134 gr/L). SIR method was carried out at 60% of WC0.33 and 25 °C during 6 h, to ensure microbiological soil response was not limited by temperature, substrate, or water. Afterwards, CO_2 concentration on each sample was measured and from this value we determined microbiological biomass by using the Eq. (4) proposed by (Anderson and Domsch 1978):

$$MB\ (\mu g g^{-1}\ soil) = 32.8 * CO_{2SIR}\ (\mu l\ CO2\ g^{-1} soil\ h^{-1}) + 3.7 \quad \text{(Eq.5)}$$

where MB is the microbial biomass and CO_{2SIR} is the CO_2 concentration obtained from SIR analysis in µl CO_2 g^{-1}soil h^{-1}.

Data analysis

As a preliminary step before data analysis, a correlation analysis was performed to explore the relationships among altitude, climatic variables, and AI. By doing this, we found that all climatic variables and AI were strongly correlated with altitude (R2 > 0.9). As we moved from lower to upper areas of both altitudinal-aridity gradients there was an increase in AI, as a result of the increase in mean annual precipitation and the decrease in mean annual temperature and maximum daily temperature (Table 2). For this reason, and because altitude usually has lower uncertainty than the interpolated climatic variables obtained from regional and global dataset, we used altitude as surrogate of aridity along the two altitudinal-aridity gradients in subsequent analysis.

	Altitude	AI	PP	Tmax
Altitude	-	-	-	-
AI	0.94 (**p < 0.05**)	-	-	-
PP	0.94 (**p < 0.05**)	0.93 (**p < 0.05**)	-	-
Tmax	-0.27 (p = 0.21)	-0.15 (p = 0.48)	-0.3 (p = 0.15)	-
Tmean	-0.94 (**p < 0.05**)	-0.85 (**p < 0.05**)	-0.88 (**p < 0.05**)	0.55 (**p < 0.05**)

Table 2 Correlation coefficients between climatic variables (PP, Tmax and Tmean), aridity index (AI) and altitude. AI: Aridity Index (dimensionless), PP: Mean annual precipitation (mm), Tmean: Mean annual temperature (°C) and Tmax: The annual mean of maximum temperatures (°C) Values in bold shown significant relationships (p < 0.05)

The effects of altitude and lithology on vegetation cover and on the three indices describing the spatial structure of vegetated and open soil patches were analysed by applying general linear models (GLMs) using lithology (limestone or mica schist) as the fix factor and altitude as the continuous predictor. As our main objective was to analyse the interaction between aridity and lithology, we explored all possible models resulting from the combination of altitude, lithology, and the interaction between them, selecting the most plausible one according to the Akaike information criterion (AIC) value using the Stats package in R (R version 4.0.2). Before data analysis we tested data normality assumption by applying the Shapiro-Wilks test.

The influence of lithology and altitude on the perennial plant community composition (relative abundance of the different species) was tested using a Permutational Multivariate

Analysis of Variance (PERMANOVA). In addition, a non-metric multidimensional scaling ordination (NMDS) of the relative abundance of the different species was done. The maximum number of interactions was established at 500 and the Bray–Curtis method was used to determine species composition similarity/dissimilarity between study areas. From NMDS results, Spearman non-parametric coefficients were calculated between NMDS axis and environmental descriptors of gradients (climatic variables, AI, altitude). Both, PERMANOVA and NMDS ordination were performed in the Vegan package (Oksanen et al. 2020) in R. Biodiversity metrics along the two altitudinal-aridity gradients were also explored by performing boxplots for each study area.

Differences in soil properties between study areas were tested using a one-way ANOVA and the Tukey's Honest Significant Difference method (Supplementary Materials Fig. S1). For AW, the averaged value of each plot was also determined. Finally, the effect of aridity and lithology on MB was determined using a GLM analysis considering lithology as the fix factor, the altitude as the predictor and the interaction between both.

Results

Changes in vegetation cover and spatial structure along altitudinal-aridity gradients

The analysis of vegetation maps derived from UAVs showed significant changes in the area covered by vegetation and bare soil along the altitudinal-aridity gradient in both lithologies (mica schist and limestone). As expected, vegetation cover increased from lower (more arid) to higher (more humid) areas on both gradients. More precisely, it ranged from 39.4% in the lower areas to 76.9% at the top of the limestone gradient and from 38.1% to 80.1% on the mica schist one. The area covered by bare soil showed the opposite pattern, with decreasing values in response to increasing aridity along the two altitudinal gradients (Fig. 2A). Even though at any given altitude, vegetation cover was always greater on the limestone gradient, lithology and its interaction with aridity had no effect on vegetation cover, and altitude (i.e., aridity) was the only factor significantly affecting the cover of vegetation and bare soil (Table 3).

The spatial structure of vegetation and soil patches also changed along altitudinal-aridity gradients. As vegetation cover increased with altitude, the mean area of vegetated patches and the value of the aggregation index also did, whereas patch circularity decreased (Fig. 2B–D). Soil patches were the opposite pattern, with decreasing size and aggregation index

values and a progressive increase in circularity. Similar to vegetation coverage, the various indices describing the spatial structure of vegetation and soil patches were significantly influenced by altitude, whereas the effect of lithology and its interaction with aridity were weak and not significant in most cases, with the exception of the aggregation index for vegetated patches (Table 3 and Fig. 2).

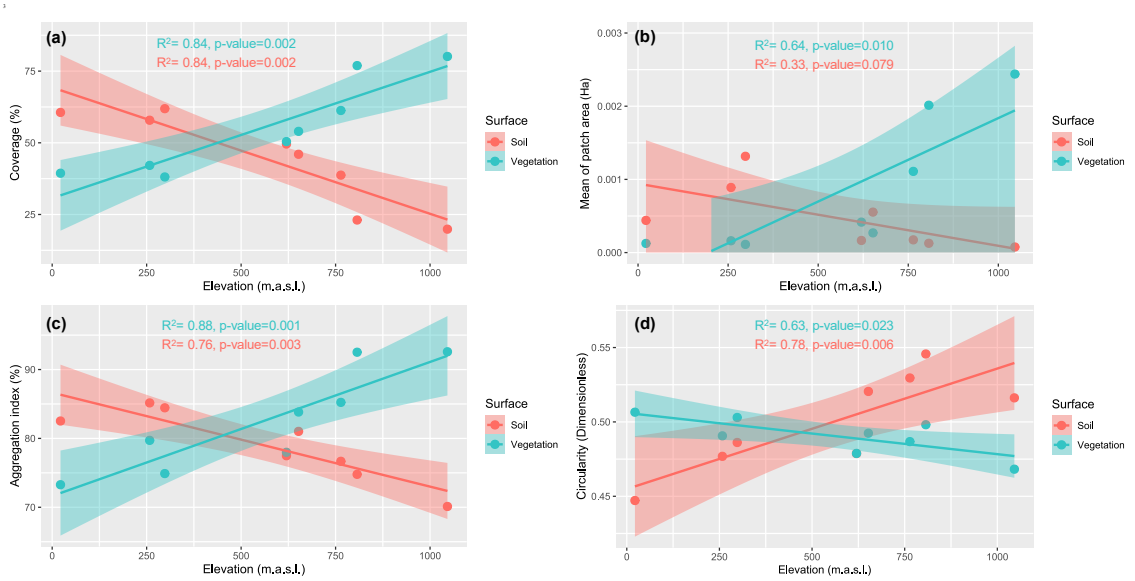

Fig. 2 Relationships between the coverage and spatial metrics of vegetated and soil patches and the altitude and lithology along study areas. Solid lines represent de GLM adjusted for each index while shadow areas represent the standard error (blue: vegetation, red: soil patches).

Vegetation composition, richness, and diversity along altitudinal-aridity gradients

Perennial plant species identified during the field surveys are shown in Supplementary Materials, Table S1. Thirty-seven perennial plant species were identified along the entire limestone gradient, ranging from 12 species in plot L3 to 18 in the highest plot (L1). Mica schist gradient shows a similar number of species (30 species), ranging from 7 species in M2 to 15 species in M4. PERMANOVA results, show that species composition varied with altitude (i.e., aridity) and lithology, and the interaction between these two factors was also significant, which means that the effect of aridity differed in the two lithologies (Table 4). This is also observed in the NMDS ordination (stress value = 0.187) where a clear effect of altitude and lithology on plant composition appeared (Fig. 3). Although *M. tenacissima* was present in all the study areas and another 13 perennial plant species were also common to both lithologies, the rest of the species differed between the gradients.

Vegetation patches	Coverage			Aggregation index			Circularity			Mean of patch area		
	F	p-value	Partial eta square	F	p-value	Partial eta square	F	p-value	Partial eta square	F	p-value	Partial eta square
Altitude	36.33	**0.002**	0.883	47.86	**0.001**	0.917	10.43	**0.023**	0.676	13.45	**0.010**	0.692
Lithology	2.35	0.186	0.320	7.46	**0.041**	0.599	-	-	-	-	-	-
Interaction	-	-	-	-	-	-	3.61	0.116	0.419	-	-	-
Soil patches												
Altitude	36.33	**0.002**	0.883	22.71	**0.003**	0.791	21.71	**0.006**	0.813	4.46	0.079	0.426
Lithology	2.35	0.186	0.320	-	-	-	-	-	-	-	-	-
Interaction	-	-	-	-	-	-	4.75	0.081	0.487	-	-	-

Table 3 Summary of General Lineal Models (GLMs) of the coverage and spatial metrics of vegetated and soil patches in response to altitude, lithology, and their interaction along the two altitudinal-aridity gradients. Values in bold shown significant relationships (p value < 0.05) and the eta-square value represent the relative importance of each factor.

On the limestone gradient, species such as *Thymus hyemalis* Lange, *Helianthemum almeriense* Pau or *Teucrium sp*. were common in the lower study areas, while they tended to be replaced in the higher areas by other species such as *Thymus baeticus* Lacaita, *Cistus clusii* Dunal, *Fumana thymifolia* (L.) Webb or *Phlomis purpurea* L. (see Supplementary Materials, Table 1 for details). The lower and more arid study areas of the mica schist gradient were characterized by the presence of species such as *Launaea lanifera* Pau, *Anthyllis cytisoides* L., *Sedum sediforme* (Jacq.) Pau or *Staehelina dubia* L. and they were replaced by species such as *Asphodelus sp*., *Retama sphaerocarpa* (L.) Boiss or *Genista umbellate* (L'Hér.) Dum. Cours in the higher, more humid study areas. *M. tenacissima* abundance also decreased from the lower to higher areas on both altitudinal aridity gradients (Supplementary Materials, Table 1).

Permanova analysis		Relative abundance	
	R^2	F	p value
Altitude	0.18	5.05	**0.01**
Lithology	0.14	6.93	**0.01**
Interaction	0.15	5.61	**0.01**

Table 4 Summary of PERMANOVA analysis of the effects of altitude, lithology, and their interaction on the plant community composition. Values in bold show significance relationships (p value < 0.05).

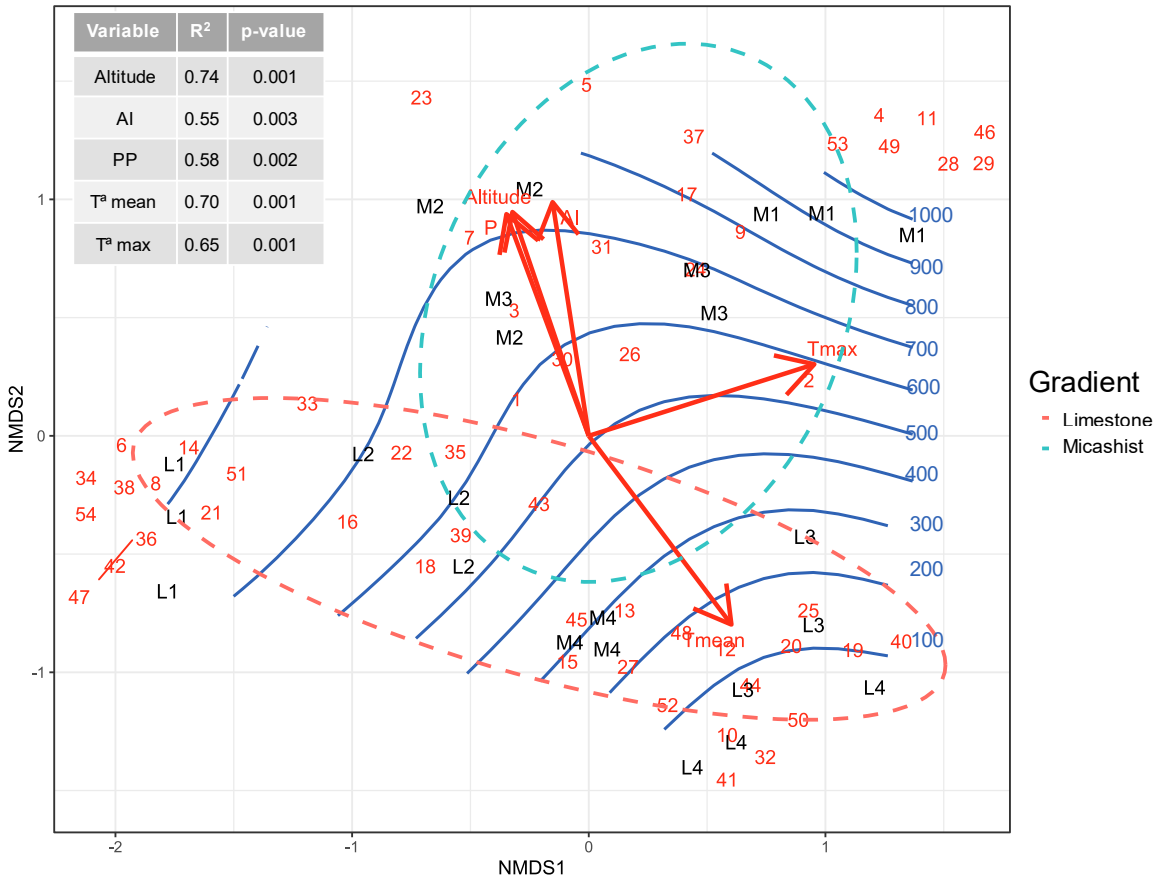

Fig. 3 NMDS ordination of perennial plant species detected in the 8 study areas during field surveys. Each field transect is represented by the name of the study area while red numbers represent plant species (see Supplementary Materials, Table 1 for details). Dotted ellipses represent limestone (orange) and mica schist (blue) lithologies and red arrows the trend of change of the climatic variables. Changes in altitude (m.a.s.l.) are symbolized by blue contour lines.

Plant diversity and richness also varied in response to aridity on both lithologies (Fig. 4). The three diversity metrics studied (H′, J, S) showed an increasing trend along the altitudinal-aridity gradient on the limestone lithology, where the highest plots were the most diversified. On the mica schist gradient however, the relationship between the different test indices and altitude was not clear, as there was very little diversity in plot M2 plot compared with the rest (Fig. 4).

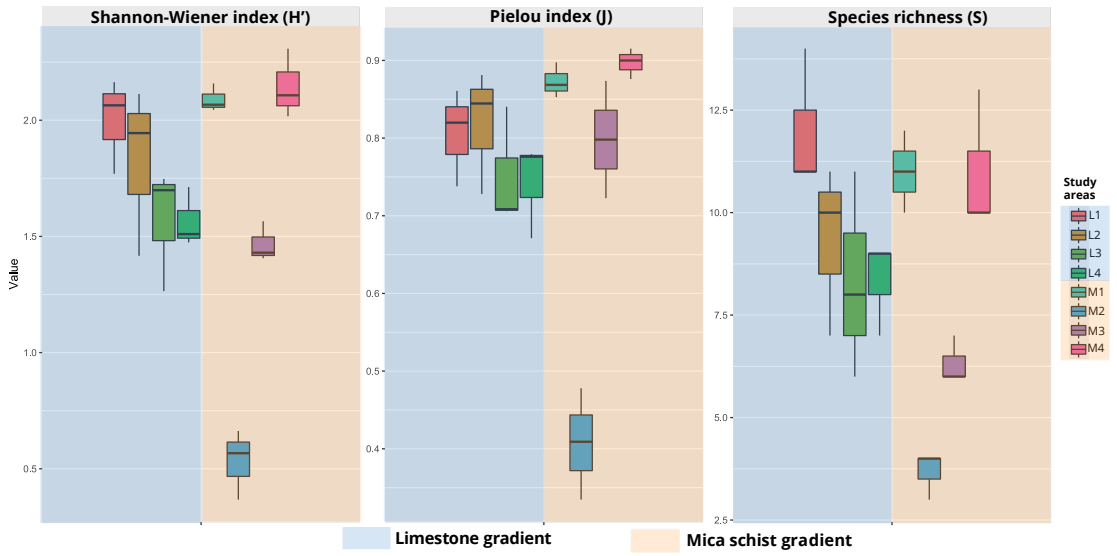

Fig. 4 Boxplots representing the median values with upper and lower quartiles of diversity metrics of the different plots on each study area derived from fields surveys. Whiskers represent the range or the variability outside the quartiles. Background colours symbolize lithology (blue: limestone, orange: mica schist).

Changes in soil properties along the altitudinal-aridity gradients

Overall, lithology, altitude and their interaction had a clear effect on soil physicochemical properties (see Supplementary Materials, Fig. S1 and Table S2). Fine particles (clay and silt) were higher in the limestone soil than in the mica schist soils and they decreased in the limestone soils as aridity increases, whereas in the mica schists soils no change have been shown in response to aridity. As a consequence, water retention capacity was stronger in the limestone gradient than in the mica schist at both pressures WC0.33 (0.33 atm) and WC15 (15 atm) and tended to decrease as aridity increases in both lithologies. On the contrary, Bulk density was greater in most arid areas and in the mica schist gradient where sand content was higher (Supplementary Materials, Fig. S1). Soil organic carbon (SOC) was higher in the limestone gradient than in the mica schist and decreased with increasing aridity in both altitudinal aridity gradients. The decreases in SOC from higher to lower areas on the altitudinal aridity gradient is more pronounced in the mica schist gradient than in limestone soils (Supplementary Materials Table S2).

According to the GLM results, MB in the soil under *M. tenacissima* canopies is was significantly affected by altitude-aridity, lithology and their interaction (GLM analysis: $R^2 = 0.74$, p value < 0.05; Table 5). Whereas MB in the limestone gradient was ~ 220 µg

g^{-1} soil in all study areas (ranging from 55 to 470 µg g^{-1}soil), MB in the mica schist gradient increased with altitude (aridification) (Fig. 5). As a result, while soil MB under M. tenacissima tussocks located in the most arid plots of the two altitudinal gradients were very similar, the highest mica schist plot it was about four times greater (~750 ± 228 µg g^{-1}soil) than in uppermost limestone plot (~ 175 ± 50 µg g^{-1}soil) (Fig. 5).

	MB		
	F	p value	Partial eta-square
Altitude	221.17	**<0.05**	2.25e−05
Lithology	23.52	**<0.05**	4.08e−01
SOC	112.37	**<0.05**	3.02e−01
Interaction	46.95	**<0.05**	2.57e−01

Table 5 Summary of General Lineal Models (GLMs) between soil microbial biomass under plant canopy (MB) and altitude, lithology, and their interactions along study areas. Values in bold show significance relationships (p value < 0.05). Partial eta-square showed the magnitude of the effect.

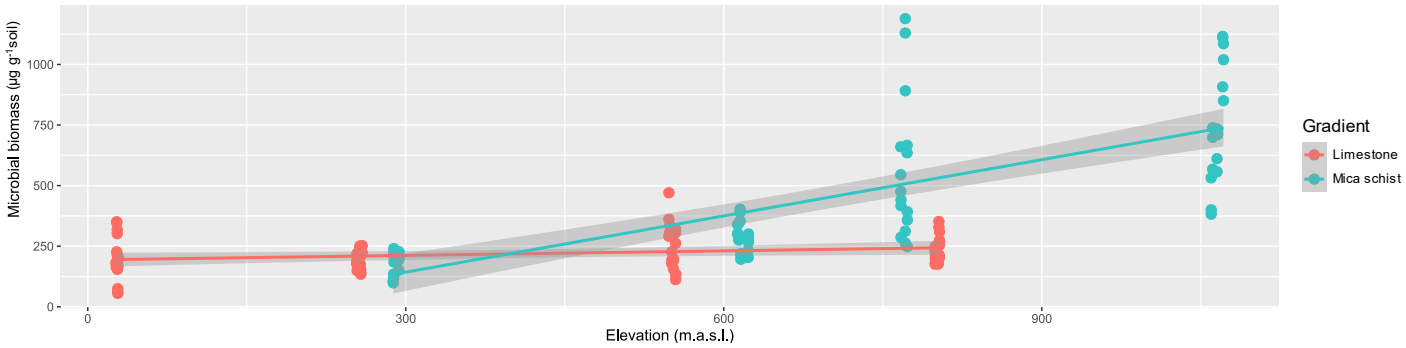

Fig. 5 Relationships between estimated microbial biomass (µg g^{-1}soil) under plant canopy with altitude over the two altitudinal-aridity gradients. Limestone gradient is represented by red colour while the mica schist one is represented in blue.

Discussion

Dryland species are morphologically and physiologically adapted to survive under the harsh environmental conditions characterising these ecosystems (Noy-Meir 1973). This is the case of *M. tenacissima*, which overcomes water scarcity by maintaining a large proportion of dead leaves (necromass) in the tussock (Rodríguez-Lozano et al. 2021). Necromass protects green leaves and the underlying soil from incoming solar radiation, reducing water loss from transpiration and evaporation (Maestre et al. 2007). Other physiological and morphological adaptations, such as shallow roots, stomata located on the underside of leaves and protected by pubescent epidermis, and the ability of leaves to curl up during dry periods, protect the plant from desiccation (Maestre et al. 2007;

Ramírez et al. 2007b). These adaptations, as well as the spatial distribution of plants maximising runoff interception, ensure survival of vegetation during the long hot dry periods that characterise these regions (Puigdefábregas 2005; Ramírez et al. 2007a). Run-on redistribution from open areas to vegetated patches in *M. tenacissima* steppes not only supplies water and nutrients to plants, but also promotes changes in the underlying soil that increase its water holding capacity, soil organic carbon content and nutrient cycling through microbial activity under the plant canopy (Gauquelin et al. 1996; Pugnaire and Haase 1996), making *M. tenacissima* tussocks resource islands that facilitate the growth and survival of other plant species and soil microorganisms (Reynolds et al. 1999; Maestre et al. 2001, 2003; Maestre and Cortina 2002). However, in spite of its mechanisms and adaptations for coping with aridity, recent studies have suggested that aridification may lead to a reduction in the overall range and productivity of *M. tenacissima* steppes by the end of the century (Vicente-Serrano et al. 2012; Ghiloufi et al. 2016; Ben Mariem and Chaieb 2017). As already described in other dryland ecosystems (Berdugo et al. 2022), our results show that this could be the result of the negative response of soil microbial communities and vegetation to more limited water availability. Moreover, the negative response of soil microbial communities and vegetation observed is modulated by the legacy of lithology on soil properties. Soil microbial biomass (Fig. 5) and vegetation composition (Fig. 3) on the two different altitudinal aridity gradients showed contrasting responses to aridification, which may have important implications for the spatial pattern of vegetated patches and system ecohydrological functioning.

According to Berdugo et al., (2022), the first and most visible effect of aridification in global drylands is a decline in vegetation productivity. This is followed by soil disruption as a direct consequence of water scarcity for soil processes and microorganisms, and indirectly as a result of the impact of aridity on plant-derived organic inputs into the soil, which diminish as a consequence of the decline in plant productivity (Delgado-Baquerizo et al. 2013, 2016; Maestre et al. 2015, 2016; Plaza et al. 2018; Moreno-Jiménez et al. 2019; Hanan et al. 2021; Berdugo et al. 2022). In agreement with these findings, our results show that aridification reduced the amount of SOC, and the soil water retention capacity, whereas bulk density increased with aridity (Supplementary Materials, Fig. S2). In the most arid areas, the loss of fine particles from increased water and wind erosion in response to the reduced vegetation cover (Wang et al. 2016) could potentially contribute to this pattern as well. It is also worth mentioning that the reduction in SOC with increased

aridity was more relevant in the mica schist altitudinal-aridity gradient than in the limestone one (Supplementary Materials Table S2). This suggests that different plant composition on the gradients along with contrasting soil water retention capacity and residence time, promote different soil organic carbon dynamics in soil.

SOC response to the combined effect of lithology and aridification was consistent with the response of soil microbial communities to both factors. For example, in our study areas coarser and darker mica schist soil, had a lower water retention capacity (Supplementary Materials, Fig. S1). As water is the main limiting factor for soil microbial activity in drylands (Rey et al. 2011), this could cause microbial communities inhabiting these soils to be less resistant and resilient in a climate change context than those in limestone soils (Lal 2020). Thus, whereas MB generally decreased with increasing aridity along the mica schist gradient, it was not affected by aridity in the limestone gradient (Fig. 5). However, MB was lower in limestone than on the mica schist gradient, mainly in high altitude plots (Fig. 5). This was unexpected as water retention capacity and available water were higher in the limestone soils (Supplementary Materials, Fig. S1). This could be explained by the differences in the soil microbial community induced by the interaction of different plant composition and water dynamics between limestone and mica schist soils (Fig. 4). Different plant species provide different organic carbon inputs into soil (Ibáñez et al. 2014; Throop et al. 2020), thus configuring SOC pools with contrasting proportions of labile and recalcitrant carbon and complexity. These differences in SOC pools along with the variability in water availability between lithologies, constrain the activity of soil microorganisms and configure different ecological carbon acquisition strategies as proposed by Morrissey et al. (2023). Soils of the mica schist gradient induces faster soil water loss from evaporation and less water retention with respect to the limestone gradient. As a result, water residence times in the mica schist soils are shorter. This may favour the presence of microbial communities adapted to easily assimilable carbon forms such as glucose, which is the substrate used in SIR measurements. This behaviour is especially relevant in study areas at higher altitudes where SOC pools are larger, evaporation is lower and the differences in plant composition are more prominent. However, further analysis with different substrates is needed to confirm this hypothesis.

The detailed analysis of vegetation composition along the two different altitudinal aridity gradients revealed over 54 perennial plant species (Supplementary Materials, Table S1). This wide variety of species, which provides a heterogenous organic matter pool for soil communities, was not homogenous along the two gradients and varied in response to aridity and lithology, as it is also affected by the interaction between these two factors. Species richness, diversity and evenness increased as aridity decreased and resources became less restrictive (Fig. 3), coinciding with previous results from other drylands (Ulrich et al. 2014; Bekai et al. 2019). Aridification and its interaction with lithology legacies also modulated the life form and plant traits in both altitudinal aridity gradients. Species composition in the most arid areas of both gradients was mainly determined by aridity tolerance, with predominance of small species, such as *Helianthemum almeriense* Pau, *Thymus hyemalis* Lange, *Launaea lanifera* Pau or *Sedum sediforme* (Jacq.) Pau. (Supplementary Materials, Table 1), well adapted to drought and high insolation, and not very selective for lithology. From lower to the higher of the two altitudinal-aridity gradients, water and nutrient availability for plants increased, and shrub species were larger with more cover. In this situation, lithology interacts with aridity promoting higher differentiation in species composition between both gradients. For example, in higher areas of the limestone gradient, species such as *Phlomis purpurea* L., *Cistus clusii* Dunal, *Ulex parviflorus* Pourr or *Fumana thymifolia* (L.) appear, which usually show predilection for basophilic soils that are common in limestone lithologies. Species with dense and extensive superficial root system able to use water stored in the soil surface were also common (e.g., *Brachypodium retusum* (Pers.) P. Beauv.), as well as species adapted to the relatively high salt concentrations (e.g., *Frankenia corymbosa* Desf., *Hammada articulata* (Moq.) O. Bolòs & Vigo, *Salsola genistoides* Poiret and *Salsola oppositifolia* Desf). The higher carbonate content common in limestone soils usually increases salt content in the surface layer, as corroborated by the average conductivity of soils on the limestone altitudinal-aridity gradient (0.29 ± 0.31 dS/m), whereas the average was lower (0.12 ± 0.06 dS/m) in mica schist soils. On the other hand, species such as *Retama sphaerocarpa* (L.) Boiss, and grasses morphologically adapted for acquiring and storing water during dry periods (i.e., *Thapsia sp*. and *Asphodelus sp*.) were common on the mica schist gradient, where water limitation is longer and more intense. For example, *Retama sphaerocarpa* (L.) Boiss, is characterised by a deep pivotal root system that may be functional more than 20 m deep (Haase et al. 1996), and can thus follow the

characteristic rock foliation of mica schist to reach deeper water, while *Asphodelus sp*. and *Thapsia sp*. use their roots to hold water during wet periods, making these species more independent of soil surface moisture.

Finally, as in other dryland ecosystems (Ghiloufi et al. 2016; Berdugo et al. 2022), our results showed an overall trend of decreasing plant cover and increasingly open bare areas from the wettest (high altitude) to the most arid study plots (low altitude) (Fig. 2A). As biotic competition for the limited water resources increases and the photosynthetic activity, cover, and biomass of vegetation decrease (Berdugo et al. 2020), the spatial arrangement of vegetation also changes (Fig. 2). Previous studies have described significant changes in the size distribution of vegetated patches in response to aridification (Kéfi et al. 2007; Scanlon et al. 2007; Berdugo et al. 2017; Meloni et al. 2017, 2019; Génin et al. 2018). However, these studies were based on isolated field samplings which can only provide information on the existing situation, or traditional remote sensing imagery, which cannot correctly characterize the inherent spatial heterogeneity of *M. tenacissima* steppes, as the pixel size is frequently larger than the size of most of individual patches (Rodríguez-Caballero et al. 2014). Consequently, most small patches are underestimated (Meloni et al. 2019). We overcame this limitation by using very high-resolution vegetation maps derived from UAV imagery (20-cm resolution). This also made it possible to go a step further and measure other important spatial metrics, such as patch shape and aggregation or connectivity between patches. These spatial indicators are strongly related to the ecohydrological functioning of *M. tenacissima* steppes and cannot be properly evaluated at the spatial resolution of

Finally, as in other dryland ecosystems (Ghiloufi et al. 2016; Berdugo et al. 2022), our results showed an overall trend of decreasing plant cover and increasingly open bare areas from the wettest (high altitude) to the most arid study plots (low altitude) (Fig. 2A). As biotic competition for the limited water resources increases and the photosynthetic activity, cover, and biomass of vegetation decrease (Berdugo et al. 2020), the spatial arrangement of vegetation also changes (Fig. 2). Previous studies have described significant changes in the size distribution of vegetated patches in response to aridification (Kéfi et al. 2007; Scanlon et al. 2007; Berdugo et al. 2017; Meloni et al. 2017, 2019; Génin et al. 2018). However, these studies were based on isolated field samplings which can only provide information on the existing situation, or traditional

remote sensing imagery, which cannot correctly characterize the inherent spatial heterogeneity of *M. tenacissima* steppes, as the pixel size is frequently larger than the size of most of individual patches (Rodríguez-Caballero et al. 2014). Consequently, most small patches are underestimated (Meloni et al. 2019). We overcame this limitation by using very high-resolution vegetation maps derived from UAV imagery (20-cm resolution). This also made it possible to go a step further and measure other important spatial metrics, such as patch shape and aggregation or connectivity between patches. These spatial indicators are strongly related to the ecohydrological functioning of *M. tenacissima* steppes and cannot be properly evaluated at the spatial resolution of available resources. Our results could also have been affected by the small number of study areas per lithology type analysed (only four sites on each gradient) and by the limited range of aridity in them. The most drastic decline in vegetation coverage induced by aridification is expected to occur during ecosystem breakdown, which has been described on the edge between semiarid and arid climates (Berdugo et al. 2022), corresponding to the most arid place included in this study. However, differences in soil texture modified the occurrence of aridity thresholds in multiple ecosystems attributes (Li et al. 2023). Therefore, it is also possible that lithology could modulate ecosystem resistance to aridification by controlling soil texture and related hydrological properties, thus promoting (i.e., mica schist soils) or buffering (limestone soils) the occurrence of this threshold. However, we could not corroborate this, as the threshold of ecosystem disruption is not within the time ranges represented at our study sites.

Current climate studies forecast a global increase in aridity due to global change that will be especially critical in the Mediterranean region (Giorgi and Lionello 2008; Lionello et al. 2014). In the Mediterranean, the IPCC predicts an increase in the mean annual temperature of 2–5 °C by the end of the century, with an increase in ETP and longer droughts. All these changes, are expected to promote a cascade of negative effects altering ecosystem functioning by limiting soil carbon pools, modifying soil microbial activity, and decreasing vegetation cover and diversity (Zeng et al. 2021; Berdugo et al. 2022) as well as changing vegetation spatial patterns (Meron 2018). According to our results, the lithological legacy plays a key role in controlling not only the individual response of ecosystem components (vegetation, soil microorganisms, etc.) and traits to climate change, but also all their potential feedback mechanisms. All these complex interactions between climate, lithology and the different ecosystem components will also interact with

changes in the system's ecohydrological functioning due to variations in the spatial structure of vegetation (Mayor et al. 2008; Okin et al. 2015). This in turn will determine ecosystem resistance and resilience to climate change and induce them to tipping points that could shift the ecosystem to a degraded state. Thus, the effects of lithology must be considered in management plans and adaptation strategies aimed at preventing the negative impact of climate change. For example, the integrative response of the plant soil system between different lithologies should be considered in future naturalization and restoration activities for climate change mitigation and adaptation, and in management of human activities that determine the response of the system to aridification (e.g., grazing; Li et al. 2023).

Conclusions

Our results demonstrate that a combination of UAV images, field and laboratory work provides a better understanding of the effect of aridification and its interaction with lithological legacies on soil properties determining water availability to biological activity in drylands. UAV images make this possible by providing spatially continuous ecosystem-level information with spatial resolution sufficient to correctly delimit the small patches that are frequently undersampled by the analysis of available free remote sensing images. Using this method, we found that aridification in *M. tenacissima* steppes reduces vegetation cover and perennial plant diversity and promotes changes in the plant community composition and the spatial distribution of vegetation in the landscape. Although lithology showed only a low direct effect on the response of vegetation cover and spatial structure by modulating soil properties related to water availability, its interaction with climatic drivers (aridity) is crucial to ecosystem resilience, as it modulates plant community composition and adaptations and the response of the underlying microbial soil biomass to aridification, potentially affecting also nutrient cycling for the vegetation and reflecting the complex interactions that govern dryland functioning. Microbial soil communities in limestone soils, which are characterised by higher water-holding capacity, do not vary in response to variations in aridity, suggesting that lithological legacies can cushion water limiting conditions for biological activity by promoting other carbon assimilation strategies that make soil functionality less dependent on the following water input. Thus, lithology should be considered in future studies on drylands response to aridification and in predictive models aimed at elucidating the

response of drylands to ongoing climate change, not only because of their direct effect on soil microbial populations, but also due to their indirect effect on the response of vegetation by altering plant nutrient cycling.

Acknowledgements

We want to acknowledge Manuel Sánchez Robles and Jose Luis Molina for their advice during field surveys and posterior plant identification, Carlos Urueta Urueta for his contribution to soils sampling and Manuel Salvador Ramón for his assistance during soil analysis in the laboratory. We also want to express our gratitude to Cecilio Oyonarte for his support and help during microbial biomass analysis.

Author contributions

BRL, ERC and YC carried out the conceptualization. BRL, EGL and JFMS performed field surveys and laboratory analysis. ERC and JFMS performed the processing of UAV images. BRL, ERC, YC done data analyses. YC and ERC were responsible for the funding acquisition. BRL wrote the original draft and developed the figures. All authors contributed to the review and editing.

Funding

This research was funded by the RH2O-ARID (P18-RT-5130) project founded by the Junta de Andalucia with European Union funds for regional development and the CRUST R-Forze (PID2021-127631NA-I00) projects funded by FEDER/Ministerio de Ciencia e Inovacion-Agencia Estatal de Investigación; and the (UAL2020-RNM-2051) project I + D + I UAL-FEDER", funded by the FEDER Andalucía 2014–2020 through the Spanish National Plan for Research and the European Union, including European Funds for Regional Development. This paper is also part of the project TED2021- 132332B-C21 funded by MCIN/AEI/https:// doi. org/ 10. 13039/50110 00110 33 and European Unión "NextGenerationEU"/ PRTR. BRL was funded by the FPU predoctoral fellowship from the Educational, Culture, and Sports Ministry of Spain (FPU17/01886). ERC was supported by the Ramon y Cajal fellowship (RYC2020-030762-I). JFMS was funded by a predoctoral grant from the University of Almeria (CPRE2023-045).

Data availability

The data used in these analyses are available from the corresponding author upon reasonable request.

Declarations

Conflict of interest The authors declare that they have no conflict of interest.

Consent for publication

All authors are aware of this submission and consent to this manuscript being published in Landscape Ecology.

References

Ackerly D (2003) Canopy gaps to climate change – extreme events, ecology and evolution. New Phytol 160:1–2

Aidoud A (2006) Les steppes arides du nord de l'Afrique. Sci Chang Planétaires / Sécheresse 17(1–2):19–30

Al-Ali ZM, Abdullah MM, Asadalla NB, Gholoum M (2020) A comparative study of remote sensing classification methods for monitoring and assessing desert vegetation using a UAV-based multispectral sensor. Environ Monit Assess 192:1–14

Anderson JPE, Domsch KH (1978) A physiological method for the quantitative measurement of microbial biomass in soils. Soil Biol Biochem 10:215–221

Bailey VL, Peacock AD, Smith JL, Bolton J (2002) Relationships between soil microbial biomass determined by chloroform fumigation-extraction, substrate-induced respiration, and phospholipid fatty acid analysis. Soil Biol Biochem 34:1385–1389

Bautista S, Mayor ÁG (2021) The role of ecohydrological (dis) connectivity in dryland functioning and management. Ecosistemas 30:1–10

Bekai F, Kadik L, Nedjimi B (2019) Effects of deferring grazing on the floristic diversity of Stipa tenacissima Loefl. Ex L. rangelands in central Algerian steppe 363–370. https://doi.org/10.1111/aje.12614

Ben Mariem H, Chaieb M (2017) Climate change impacts on the distribution of stipa tenacissima l. Ecosystems in north african arid zone - a case study in tunisia. Appl Ecol Environ Res 15:67–82

Berdugo M, Delgado-Baquerizo M, Soliveres S et al (2020) Global ecosystem thresholds driven by aridity. Science (80-) 367:787–790

Berdugo M, Gaitán JJ, Delgado-Baquerizo M, Crowther TW, Dakos V (2022) Prevalence and drivers of abrupt vegetation shifts in global drylands. PNAS 119:43

Berdugo M, Kéfi S, Soliveres S, Maestre FT (2017) Plant spatial patterns identify alternative ecosystem multifunctionality states in global drylands. Nat Ecol Evol 1:1–7

Berghuis PMJ, Mayor ÁG, Rietkerk M, Baudena M (2020) More is not necessarily better: the role of cover and spatial organization of resource sinks in the restoration of patchy drylands. J Arid Environ. https://doi.org/10.1016/j.jaridenv.2020.104282

Bonkoungou EG (2001) Biodiversity in drylands: challenges and opportunities for. Glob Drylands Partnersh 1–20 Brandt M, Hiernaux P, Rasmussen K et al (2019) Changes in rainfall distribution promote woody foliage production in the Sahel. Commun Biol 2:1–10

Cantón Y, Solé-Benet A, de Vente J et al (2011) A review of runoff generation and soil erosion across scales in semiarid south-eastern Spain. J Arid Environ 75:1254–1261

Cherlet M, Hutchinson C, Reynolds J et al (2018) World atlas of desertification. Publications Office of the European Union JRC, Luxembourg

Company J, Valiente N, Fortesa J et al (2022) Secondary succession and parent material drive soil bacterial community composition in terraced abandoned olive groves from a Mediterranean hyper-humid mountainous area. Agric Ecosyst Environ. https://doi.org/10.1016/j.agee.2022.107932

D'Odorico P, Bhattachan A (2012) Hydrologic variability in dryland regions: impacts on ecosystem dynamics and food security. Philos Trans R Soc B Biol Sci 367:3145–3157

D'Odorico P, Caylor K, Okin GS, Scanlon TM (2007) On soil moisture-vegetation feedbacks and their possible effects on the dynamics of dryland ecosystems. J Geophys Res Biogeosci 112:1–10

Dacal M, Delgado-Baquerizo M, Barquero J et al (2022) Temperature increases soil respiration across ecosystem types and soil development, but soil properties determine the magnitude of this effect. Ecosystems 25:184–198

Dawelbait M, Morari F (2008) Limits and potentialities of studying dryland vegetation using the optical remote sensing. Ital J Agron 3:97–106

Deblauwe V, Couteron P, Lejeune O, Bogaert J, Barbier N (2011) Environmental modulation of self-organized periodic vegetation patterns in Sudan. Ecography 34:990–1001

Delgado-Baquerizo M, Maestre FT, Gallardo A et al (2013) Decoupling of soil nutrient cycles as a function of aridity in global drylands. Nature 502:672–676

Delgado-Baquerizo M, Maestre FT, Gallardo A et al (2016) Human impacts and aridity differentially alter soil N availability in drylands worldwide. Glob Ecol Biogeogr 25:36–45

Gauquelin T, Jalut G, Iglesias M et al (1996) Phytomass and carbon storage in the Stipa tenacissima steppes of the Baza basin, Andalusia, Spain. J Arid Environ 34:277–286

Gee WG, Or D (2002) Particle-size analysis. In: Dane J, Topp GC (eds) Methods of soil analysis: part 4 physical methods. Soil Science Society of America USA, p 255–293

Génin A, Majumder S, Sankaran S et al (2018) Monitoring ecosystem degradation using spatial data and the R package spatialwarnings. Methods Ecol Evol 9:2067–2075

Getzin S, Löns C, Yizhaq H et al (2022) High-resolution images and drone-based LiDAR reveal striking patterns of vegetation gaps in a wooded spinifex grassland of Western Australia. Landsc Ecol 37:829–845

Ghandhi P, Iams S, Bonetti S, Silber M (2019) Vegetation pattern formation in drylands. Dryl Ecohydrol. https://doi.org/10.1007/978-3-030-23269-6_18

Ghiloufi W, Quero JL, García-Gómez M, Chaieb M (2016) Potential impacts of aridity on structural and functional status of a southern Mediterranean Stipa tenacissima steppe. S Afr J Bot 103:170–180

Giorgi F, Lionello P (2008) Climate change projections for the Mediterranean region. Glob Planet Change 63:90–104 Hanan NP, Milne E, Aynekulu E et al (2021) A role for drylands in a carbon neutral world? Front Environ Sci 9:1–10

Haase P, Pugnaire FI, Fernández EM, Puigdefábregas J, Clark SC, Incoll LD (1996) An investigation of rooting depth of the semiarid shrub Retama sphaerocarpa (L.) Boiss. by labelling of ground water with a chemical tracer. J Hydrol 177:23–31

Hesselbarth MHK, Sciaini M, With KA et al (2019) Landscapemetrics: an open-source R tool to calculate landscape metrics. Ecography 42:1648–1657

Ibáñez JJ, Zuccarello V, Ganis P, Feoli E (2014) Pedodiversity deserves attention in plant biodiversity research. Plant Biosyst 148:1112–1116

Kaneko K, Nohara S (2014) Review of effective vegetation mapping using the UAV (unmanned aerial vehicle) method. J Geogr Inf Syst 06:733–742

Kaouthar J, Chaieb M (2009) The effect of Stipa tenacissima tussocks on some soil surface properties under arid bioclimate in the southern Tunisia. Acta Bot Gall 156:173–181

Kéfi S, Rietkerk M, Alados CL et al (2007) Spatial vegetation patterns and imminent desertification in Mediterranean arid ecosystems. Nature 449:213–217

Klute A, Klute A (1986) Water retention: laboratory methods. In: Klute A, Topp (eds) Methods of soil analysis: part 1 physical and mineralogical methods. Soil Science Society of America USA, p 635–662

Lal R (2020) Soil organic matter and water retention. Agron J 112:3265–3277

Li C, Fu B, Wang S, Stringer L, Zhou W, Ren Z, Hu M, Zhang Y, Rodriguez-Caballero E, Weber B, Maestre F (2023) Climate-driven ecological thresholds in China's drylands modulated by grazing. Nat Sustain. https://doi.org/10.1038/s41893-023-01187-5

Liao C, Agrawal A, Clark PE et al (2020) Landscape sustainability science in the drylands: mobility, rangelands and livelihoods. Landsc Ecol 35:2433–2447

Lin Y, Han G, Zhao M, Chang SX (2010) Spatial vegetation patterns as early signs of desertification: a case study of a desert steppe in Inner Mongolia, China. Landsc Ecol 25:1519–1527

Lionello P, Abrantes F, Gacic M et al (2014) The climate of the Mediterranean region: research progress and climate change impacts. Reg Environ Chang 14:1679–1684

Lu N, Wang M, Ning B et al (2018) Research advances in ecosystem services in drylands under global environmental changes. Curr Opin Environ Sustain 33:92–98

Ludwig JA, Wilcox BP, Breshears DD et al (2005) Vegetation patches and runoff-erosion as interacting ecohydrological processes in semiarid landscapes. Ecology 86:288–297

Maestre F, Benito BM, Berdugo M et al (2021) Biogeography of global drylands. New Phytol 231:540–558

Maestre FT, Bautista S, Cortina J (2003) Positive, negative, and net effects in grass-shrub interactions in Mediterranean semiarid grasslands. Ecology 84:3186–3197

Maestre FT, Bautista S, Cortina J, Bellot J (2001) Potential for using facilitation by grasses to establish shrubs on a semiarid degraded steppe. Ecol Appl 11:1641–1655

Maestre FT, Cortina J (2002) Spatial patterns of surface soil properties and vegetation in a Mediterranean semi-arid steppe. Plant Soil 241:279–291

Maestre FT, Delgado-Baquerizo M, Jeffries TC et al (2015) Increasing aridity reduces soil microbial diversity and abundance in global drylands. Proc Natl Acad Sci U S A 112:15684–15689

Maestre FT, Eldridge DJ, Soliveres S et al (2016) Structure and functioning of dryland ecosystems in a changing world. Annu Rev Ecol Evol Syst 47:215–237

Maestre FT, Ramírez DA, Cortina J (2007) Ecología del esparto (Stipa tenacissima L.) y los espartales de la Península Ibérica. Ecosistemas 16:1–20

Martínez-Hernández C, Rodrigo-Comino J, Romero-Díaz A (2017) Impact of lithology and soil properties on abandoned dryland terraces during the early stages of soil erosion by water in south-east Spain. Hydrol Process 31:3095–3109

Mayor ÁG, Bautista S, Rodriguez F, Kéfi S (2019) Connectivity-mediated ecohydrological feedbacks and regime shifts in drylands. Ecosystems 22:1497–1511

Mayor ÁG, Bautista S, Small EE et al (2008) Measurement of the connectivity of runoff source areas as determined by vegetation pattern and topography: a tool for assessing potential water and soil losses in drylands. Water Resour Res 44:1–13

Mayor ÁG, Kéfi S, Bautista S et al (2013) Feedbacks between vegetation pattern and resource loss dramatically decrease ecosystem resilience and restoration potential in a simple dryland model. Landsc Ecol 28:931–942

Meloni F, Granzotti CRF, Bautista S, Martinez AS (2017) Scale dependence and patch size distribution: clarifying patch patterns in Mediterranean drylands. Ecosphere. https://doi.org/10.1002/ecs2.1690

Meloni F, Nakamura GM, Granzotti CRF, Martinez AS (2019) Vegetation cover reveals the phase diagram of patch patterns in drylands. Phys A Stat Mech Its Appl 534:122048

Meron E (2018) From patterns to function in living systems: dryland ecosystems as a case study. Annu Rev Condens Matter Phys 9:79–103

Mingorance MD, Barahona E, Fernández-Gálvez J (2007) Guidelines for improving organic carbon recovery by the wet oxidation method. Chemosphere 68:409–413

Moore JC (2013) Diversity, taxonomic versus functional. Encycl Biodivers Second Ed 2:648–656

Moreno-Jiménez E, Plaza C, Saiz H et al (2019) Aridity and reduced soil micronutrient availability in global drylands. Nat Sustain 2:371–377

Morrissey EM, Kane J, Tripathi BM et al (2023) Carbon acquisition ecological strategies to connect soil microbial biodiversity and carbon cycling. Soil Biol Biochem. https://doi.org/10.1016/j.soilbio.2022.108893

Moyano FE, Manzoni S, Chenu C (2013) Responses of soil heterotrophic respiration to moisture availability: an exploration of processes and models. Soil Biol Biochem 59:72–85

Noy-Meir I (1973) Desert ecosystems: environment and producers. Annu Rev Ecol Evol Syst 4:25–51

Okin GS, De Las Heras MM, Saco PM et al (2015) Connectivity in dryland landscapes: shifting concepts of spatial interactions. Front Ecol Environ 13:20–27

Oksanen J, Blanchet FG, Friendly M et al (2020) Vegan: community ecology package. https://CRAN.R-project.org/package= vegan

Peguero-Pina JJ, Vilagrosa A, Alonso-Forn D et al (2020) Living in drylands: functional adaptations of trees and shrubs to cope with high temperatures and water scarcity. Forests 11:1–23

Pielou EC (1966) The measurement of diversity in different types of biological collections. J Theor Biol 13:131–144

Plaza C, Zaccone C, Sawicka K et al (2018) Soil resources and element stocks in drylands to face global issues. Sci Rep 8:1–8

Prăvălie R (2016) Drylands extent and environmental issues. A global approach. Earth-Sci Rev 161:259–278 Pugnaire FI, Armas C, Maestre FT (2011) Positive plant interactions in the Iberian Southeast: mechanisms, environmental gradients, and ecosystem function. J Arid Environ 75:1310–1320

Pugnaire FI, Haase P (1996) Comparative physiology and growth of two perennial tussock grass species in a semiarid environment. Ann Bot 77:81–86

Puigdefábregas J (2005) The role of vegetation patterns in structuring runoff and sediment fluxes in drylands. Earth Surf Process Landforms 30:133–147

Puigdefábregas J, Sole A, Gutierrez L et al (1999) Scales and processes of water and sediment redistribution in drylands: results from the Rambla Honda field site in Southeast Spain. Earth Sci Rev 48:39–70

Ramírez DA, Bellot J, Domingo F, Blasco A (2007a) Can water responses in Stipa tenacissima L. during the summer season be promoted by non-rainfall water gains in soil? Plant Soil 291:67–79

Ramírez DA, Bellot J, Domingo F, Blasco A (2007b) Stand transpiration of Stipa tenacissima grassland by sequential scaling and multi-source evapotranspiration modelling. J Hydrol 342:124–133

Regüés D, Badía D, Echeverría MT et al (2017) Analysing the effect of land use and vegetation cover on soil infiltration in three contrasting environments in northeast Spain. Cuad Investig Geográfica 43:141–169

Rey A, Pegoraro E, Oyonarte C et al (2011) Impact of land degradation on soil respiration in a steppe (Stipa tenacissima L.) semi-arid ecosystem in the SE of Spain. Soil Biol Biochem 43:393–403. https://doi.org/10.1016/j.soilbio.2010.11.007

Reynolds JF, Virginia RA, Kemp PR et al (1999) Impact of drought on desert shrubs: effects of seasonality and degree of resource island development. Ecol Monogr 69:69–106

Rietkerk M, Bastiaansen R, Banerjee S et al (2021) Evasion of tipping in complex systems through spatial pattern formation. Science (80-). https://doi.org/10.1126/science.abj0359

Rodríguez-Caballero E, Chamizo S, Roncero-Ramos B et al (2018) Runoff from biocrust: a vital resource for vegetation performance on Mediterranean steppes. Ecohydrology 11:1–13

Rodríguez-Caballero E, Escribano P, Cantón Y (2014) Advanced image processing methods as a tool to map and quantify different types of biological soil crust. ISPRS J Photogramm Remote Sens 90:59–67

Rodríguez-Caballero E, Reyes A, Kratz A et al (2022) Effects of climate change and land use intensification on regional biological soil crust cover and composition in southern Africa. Geoderma. https://doi.org/10.1016/j.geoderma.2021.115508

Rodríguez-Lozano B, Rodríguez-Caballero E, Maggioli L,Cantón Y (2021) Non-destructive biomass estimation in mediterranean alpha steppes: improving

traditional methods for measuring dry and green fractions by combining proximal remote sensing tools. Remote Sens 13:1–19

Scanlon TM, Caylor KK, Levin SA, Rodriguez-Iturbe I (2007) Positive feedbacks promote power-law clustering of Kalahari vegetation. Nature 449:209–212

Shannon CE (1948) A mathematical theory of communication. Bell Syst Tech J 27:379–423

Smith WK, Dannenberg MP, Yan D et al (2019) Remote sensing of dryland ecosystem structure and function: progress, challenges, and opportunities. Remote Sens Environ 233:111401

Suggitt AJ, Wilson RJ, Isaac NJB et al (2018) Extinction risk from climate change is reduced by microclimatic buffering. Nat Clim Chang 8:713–717

Throop HL, Seely MK, Marufu VJ, Participants SDP (2020) Multiple scales of spatial heterogeneity control soil respiration responses to precipitation across a dryland rainfall gradient. Plant Soil 453:423–443

Trabucco A, Zomer RJ (2018) Global Aridity Index and Potential Evapo-Transpiration (ET0) Climate Database v2. CGIAR Consortium for Spatial Information (CGIARCSI). Publ online, available from CGIAR-CSI GeoPortal https://cgiarcsi.community

Ulrich W, Soliveres S, Maestre FT et al (2014) Climate and soil attributes determine plant species turnover in global drylands. J Biogeogr 41:2307–2319

Vicente-Serrano SM, Zouber A, Lasanta T, Pueyo Y (2012) Dryness is accelerating degradation of vulnerable shrublands in semiarid mediterranean environments. Ecol Monogr 82:407–428

Wang XG, Sistla SA, Wang XB et al (2016) Carbon and nitrogen contents in particle-size fractions of topsoil along a 3000km aridity gradient in grasslands of northern China. Biogeosciences 13:3635–3646. https://doi.org/10.5194/bg-13-3635-2016

Weltzin JF, Loik ME, Schwinning S et al (2003) Assessing the response of terrestrial ecosystems to potential changes in precipitation. Bioscience 53:941–952

Xu C, Van Nes EH, Holmgren M et al (2015) Local facilitation may cause tipping points on a landscape level preceded by early-warning indicators. Am Nat 186:E81–E90

Zeng H, Wu B, Zhang M et al (2021) Dryland ecosystem dynamic change and its drivers in Mediterranean region. Curr Opin Environ Sustain 48:59–67

Zhang DH, Li XR, Zhang F et al (2016) Effects of rainfall intensity and intermittency on woody vegetation cover and deep soil moisture in dryland ecosystems. J Hydrol 543:270–282

Publisher's Note

Supplementary

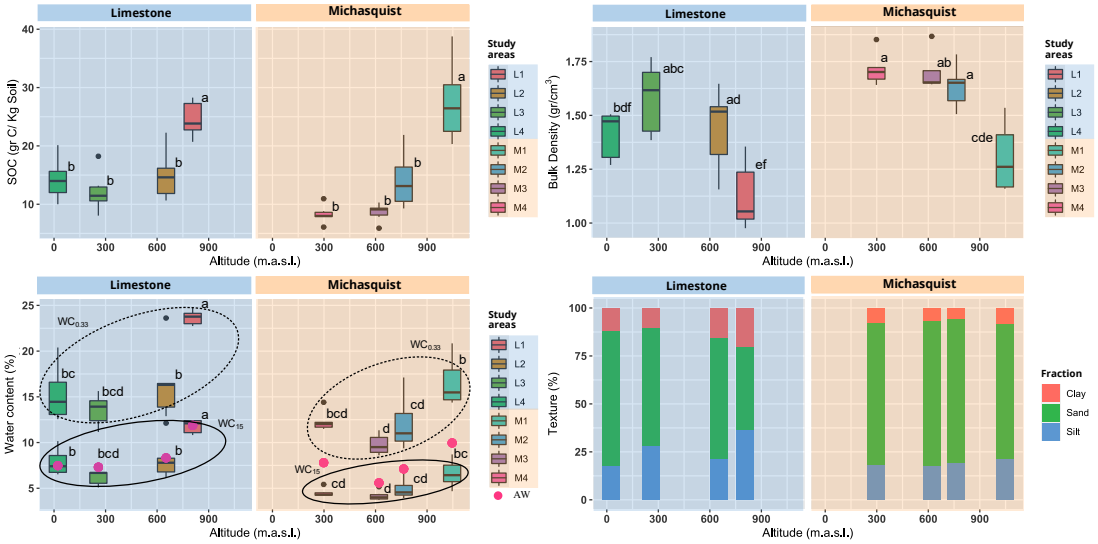

Supplementary, Fig. S1 Soil properties along the two altitudinal-aridity gradients. Pink dots represent the mean value of AW (available water) in each study hillslope.

ID	Specie	L1	L2	L3	L4	M1	M2	M3	M4
1	*Anthyllis cytisoides* L.		X					X	X
2	*Artemisia barrelieri* Besser			X	X	X		X	X
3	*Asparagus horridus* L.	X	X	X	X	X	X	X	X
4	*Asphodelus* sp.					X			
5	*Ballota hirsuta* Benth.					X	X		
6	*Brachypodium retusum* (Pers.) P. Beauv.	X							
7	*Cheilanthes acrostica* (Balbis) Tod.							X	
8	*Cistus clusii* Dunal	X	X						
9	*Eryngium campestre* L.							X	
10	*Fagonia cretica* L.				X				X
11	*Ferula communis L. subsp. catalaunica* (C. Vicioso) Sánchez *Cuxart & Berna*					X			
12	*Frankenia corymbosa* Desf.				X				X
13	*Fumana ericoides* (Cav.) Gand.								X
14	*Fumana thymifolia* (L.) Webb	X	X						
15	*Genista* sp.								X
16	*Genista spartioides* Spach	X	X						
17	*Genista umbellata* (L'Hér.) Dum. Cours	X				X			
18	*Globularia alypum* L.		X						
19	*Hammada articulata* (Moq.) O. Bolòs & Vigo			X	X				
20	*Helianthemum almeriense* Pau.			X	X				X
21	*Helianthemum syriacum* (Jacq.) Dum. Cours.	X	X						
22	*Helianthemum violaceum* (Cav.) Pers.		X						
23	*Hyparrhenia hirta* (L.) Stapf						X		
24	*Hyparrhenia* sp.	X	X						
25	*Launaea arborescens* (Batt.) Murb.			X					
26	*Launaea lanifera* Pau		X					X	X
27	*Lavandula multifida* L.								X
28	*Lavandula stoechas* L.					X			
29	*Lobularia maritima* (L.) Desv. subsp. maritima					X			
30	*Macrochloa tenacissima* (L.) Kunth	X	X	X	X	X	X	X	X
31	*Phagnalon rupestre* (L.) DC.	X				X	X	X	
32	*Phagnalon* sp.				X				
33	*Phlomis lychnitis* L.	X				X			
34	*Phlomis purpurea* L.		X						
35	*Pinus halepensis* Mill.		X						
36	*Polygala monspeliaca* L.	X							
37	*Retama sphaerocarpa* (L.) Boiss.					X	X	X	
38	*Rhamnus lycioides* L.	X							
39	*Ruta angustifolia* Pers.		X						
40	*Salsola genistoides* Poiret			X	X				
41	*Salsola oppositifolia* Desf.				X				
42	*Satureja obovata* Lag.	X							
43	*Sedum sediforme* (Jacq.) Pau		X	X			X		X
44	*Sisymbrium irio* L.			X					
45	*Staehelina dubia* L.								X

Continúa en la Pág. 89

ID	***Specie***	***L1***	***L2***	***L3***	***L4***	***M1***	***M2***	***M3***	***M4***
46	*Stipa capillata* L.					X			
47	*Teucrium pseudochamaepitys* L.	X							
48	*Teucrium* sp.	X	X	X	X				
49	*Thapsia* sp.					X			
50	*Thymelaea hirsuta* (L.) Endl.			X	X				X
51	*Thymus baeticus* Lacaita	X	X						
52	*Thymus hyemalis* Lange			X	X				X
53	*Thymus zygis L. subsp. gracilis* (Boiss.) R. Morales					X			
54	*Ulex parviflorus* Pourr.	X							

Supplementary, Table 1. Perennial plant species recorded during field transects in the different study areas along the two altitudinal-aridity gradients with contrasting lithology (L: Limestone, M: michasquist).

Soil properties	SOC (R^2 = 0.52)			$WC_{0.33}$ (R^2 = 0.50)			WC_{15} (R^2 = 0.62)			AW (R^2 = 0.33)		
	F	p-value	Partial eta square	F	p-value	Partial eta square	F	p-value	Partial eta square	F	p-value	Partial eta square
Altitude	32.60	**8.99 e-07**	0.507	6.90	**0.01183**	0.356	2.53	0.1188	0.350	10.98	**0.001851**	0.318
Lithology	14.25	**0.0005**	0.245	41.50	**7.557e-08**	0.485	75.92	**3.911e-11**	0.633	14.37	**0.0004529**	0.246
Interaction	7.57	**0.009**	0.147	1.29	0.26263	0.028	1.34	0.2535	0.029	1.02	0.318894	0.023
Soil properties	Bulk density (R^2 = 0.43)			Sand (R^2 = 0.80)			Silt (R^2 = 0.58)			Clay (R^2 = 0.89)		
	F	p-value	Partial eta square	F	p-value	Partial eta square	F	p-value	Partial eta square	F	p-value	Partial eta square
Altitude	7.03	**0.01198**	0.352	6.17	**0.01684**	0.552	6.24	**0.01629**	0.382	1.03	0.4902	0.602
Lithology	24.00	**2.173e-05**	0.407	168.69	**2.2e-16**	0.793	55.71	**2.4e-09**	0.559	370.82	**2.2e-16**	0.894
Interaction	1.03	0.31607	0.029	23.22	**1.753e-05**	0.345	7.21	**0.01020**	0.141	54.42	**3.214e-09**	0.553

Supplementary Table 2. Summary of General Linal Models (GLMs) between soil properties, altitude, lithology, and their interactions along study areas. R^2 is the value of R-squared of each GLM. Values in bold show significance relationships (p-value < 0.05). Partial eta-square showed the magnitude of the effect.